



# Acoustofluidics for biomedical applications

Joseph Rufo<sup>1</sup>, Feiyan Cai<sup>1,2</sup>✉, James Friend<sup>1,3,4</sup>✉, Martin Wiklund<sup>1</sup>✉  
and Tony Jun Huang<sup>1</sup>✉

**Abstract** | Acoustofluidic technologies utilize acoustic waves to manipulate fluids and particles within fluids, all in a contact-free and biocompatible manner. Over the past decade, acoustofluidic technologies have enabled new capabilities in biomedical applications ranging from the precise patterning of heterogeneous cells for tissue engineering to the automated isolation of extracellular vesicles from biofluids for rapid, point-of-care diagnostics. In this Primer, we explain the underlying physical principles governing the design and operation of acoustofluidic technologies and describe the various implementations that have been developed for biomedical applications. We aim to demystify the rapidly growing field of acoustofluidics and provide a unified perspective that will allow end users to choose the acoustofluidic technology that is best suited for their research needs. The experimental set-ups for each type of acoustofluidic device are discussed along with their advantages and limitations. In addition, we review typical types of data that are obtained from acoustofluidic experiments and describe how to model different forces acting on particles within an acoustofluidic device. We also discuss data reproducibility and the need to establish standards for the deposition of data sets within the field. Finally, we provide our perspective on how to optimize device performance and discuss areas of future development.

## Inviscid fluid

A fluid that has a viscosity of zero.

Acoustofluidic devices<sup>1–3</sup> combine acoustic waves with fluid dynamics to serve various applications in biomedicine<sup>4</sup>, including the manipulation of cells and particles for single-cell and single-molecule analysis, the isolation of bioparticles for point-of-care diagnostics, the automation of workflows in life science laboratories and the positioning of cells for tissue engineering. By coupling acoustic waves with fluids to generate acoustic radiation forces and acoustic streaming, acoustofluidic technologies offer a contact-free method for manipulating particles and actuating fluids. Acoustic diffraction, reflection and interference can be exploited to create well-defined pressure distributions, in turn enabling precise particle and fluid manipulation. Owing to the tuneable nature of acoustic waves and the wide range of operating frequencies used (kilohertz to gigahertz), acoustofluidic technologies can directly manipulate particles ranging from tens of nanometres to several millimetres in length. The applied acoustic powers are typically in the same range as those used in ultrasound imaging, allowing acoustofluidic devices to manipulate nanoscale bioparticles, cells and small organisms in a highly biocompatible manner.

✉e-mail: fy.cai@siat.ac.cn;  
jfriend@ucsd.edu;  
martin.wiklund@biox.kth.se;  
tony.huang@duke.edu  
<https://doi.org/10.1038/s43586-022-00109-7>

absorption that transfers linear momentum from the acoustic field to the object<sup>5–8</sup>. Based on the stress tensor proposed by Brillouin<sup>9</sup> and far-field scattering theory, the force can be expressed as the integral of the time-averaged stress tensor for the total sound field over a closed equilibrium surface  $s$  that contains the object of interest,  $\mathbf{F}_R = -\oint_s \Pi \cdot d\mathbf{s}$ . Specifically,

$$\mathbf{F}_R = -\oint_s \left[ \left( \frac{1}{2\rho_0 c_0^2} \langle p^2 \rangle - \frac{\rho_0}{2} \langle |\mathbf{v}|^2 \rangle \right) \mathbf{I} + \rho_0 \langle \mathbf{v} \mathbf{v} \rangle \right] \cdot d\mathbf{s}, \quad (1)$$

where  $\oint_s$  represents the surface integral, the area differential  $d\mathbf{s} = nd\mathbf{s}$  is directed away from the object,  $\mathbf{I}$  is the unit tensor and the angle brackets denote averaging over the sound wave period<sup>5,7,8,10–13</sup>. The quantities  $\rho_0$  and  $c_0$  are the density and the sound speed in the fluid.  $p$  and  $\mathbf{v}$  are, respectively, the total acoustic pressure and velocity that arise from the sum of waves incident on the object and scattered by it.

In principle, Eq. 1 can be used to analyse the acoustic radiation forces from arbitrary acoustic fields upon particles of arbitrary shape in an inviscid fluid. Absorption in both the object and the adjacent media can also play an important role on the force<sup>14–17</sup> and even on torques<sup>18–20</sup>. In lossy media, Eq. 1 is still a good approximation when

**Author addresses**

<sup>1</sup>Department of Mechanical Engineering and Materials Science, Duke University, Durham, NC, USA.

<sup>2</sup>Paul C. Lauterbur Research Centre for Biomedical Imaging, Shenzhen Institutes of Advanced Technology, Chinese Academy of Sciences, Shenzhen, Guangdong, China.

<sup>3</sup>Center for Medical Device Engineering and Biomechanics, Department of Mechanical and Aerospace Engineering, Jacobs School of Engineering, University of California San Diego, La Jolla, CA, USA.

<sup>4</sup>Department of Surgery, School of Medicine, University of California San Diego, La Jolla, CA, USA.

<sup>5</sup>Department of Applied Physics, Royal Institute of Technology, Stockholm, Sweden.

the thicknesses of the thermal or viscous boundary layers — layers of fluid near a channel wall in which the effects of heat or viscosity, respectively, cannot be neglected<sup>21</sup> — are small and the acoustic streaming is weak<sup>15,22</sup>. A similar approach works for determining the torque<sup>23–25</sup>.

The challenge in evaluating the above expression lies in the calculation of the scattered acoustic field. The multipole expansion method has long been used to calculate the forces upon spherical or cylindrical particles in symmetrical (planar, spherical and so on) fields<sup>11,26–29</sup>, which can effectively uncover the mechanism of the momentum transfer between the field and the particles<sup>7,17</sup>. Recently, the angular spectrum method has been used to calculate forces upon particles in holographically produced fields<sup>13,30</sup>. For more complex cases, such as particles with arbitrary shape or in a closed chamber, numerical simulations based on the finite difference method<sup>31</sup>, the Boltzmann lattice method<sup>32</sup>, the boundary element method<sup>33</sup> and the finite element method (especially via commercial software COMSOL Multiphysics)<sup>34</sup> have been proposed to determine the forces on the particles. These numerical methods are usually time and resource intensive when used for three-dimensional (3D) analyses, but they are indeed indispensable tools to understand resonance and force distribution in the whole acoustofluidic device.

If there are multiple particles in the field, the acoustic radiation force exerted on one given particle involves the acoustic interaction force from multiple scattering events from other particles. This force can also be evaluated by using Eq. 1, where the incident field in this case is the sum of the external field and the scattered fields from the other particles<sup>35–37</sup>. The multipole expansion method combined with the translational addition theorem can effectively deal with this problem<sup>35</sup>.

For acoustofluidics in biomedical applications, the manipulated objects are typically much smaller than the acoustic wavelength. For example, the radius  $a$  of a cell is usually in the range of 5–15  $\mu\text{m}$ , whereas the wavelength  $\lambda$  of a 10 MHz acoustic wave in water at room temperature is approximately 150  $\mu\text{m}$ . They can be modelled as a Rayleigh particle ( $a \ll \lambda$ ), where the scattering field is dominated by the monopole and dipole<sup>38</sup>. Gor'kov derived a simple formula to describe the forces acting on a Rayleigh particle in the situation where the wave field has a standing wave feature or, in general, has a strong spatial gradient of acoustic wave energies<sup>39</sup>. The force is formed in terms of the spatial gradient of the force potential:

$$\mathbf{F} = -\nabla U, \quad (2)$$

where the Gor'kov force potential  $U$  is given by:

$$U = \frac{4\pi a^3}{3} \left[ f_1 \frac{1}{2\rho_0 c_0^2} \langle p_{\text{in}}^2 \rangle - f_2 \frac{3\rho_0}{4} \langle |\mathbf{v}_{\text{in}}|^2 \rangle \right], \quad (3)$$

where

$$f_1 = 1 - \frac{c_0^2 \rho_0}{c_p^2 \rho_p}, \quad f_2 = \frac{2(\rho_p - \rho_0)}{2\rho_p + \rho_0}. \quad (4)$$

Here  $\rho_p$  and  $c_p$  are the density and the longitudinal wave velocity of the material used in the particle;  $f_1$  and  $f_2$  are, respectively, two acoustic strength parameters associated with the sphere's monopolar and dipolar modes; and  $\langle p_{\text{in}}^2 \rangle$  and  $\langle |\mathbf{v}_{\text{in}}|^2 \rangle$  are the time-averaged acoustic potential and kinetic energy of the incident field at the position of the particle, respectively.

Note that the force produced upon an object in a plane standing wave (usually named gradient force) is proportional to  $a^3$ , whereas the force exerted by a plane travelling wave (often called scattering force) is proportional to  $a^6$  in the Rayleigh approximation<sup>40</sup>. Thus, the forces exerted on a Rayleigh particle by an arbitrary wave field are dominated by the gradient force unless the wave field has a weak or no spatial gradient of wave energies<sup>13,41</sup>. As the size of particle decreases especially to the nanoscale, viscous and thermo-viscous effects on the acoustic radiation force need to be considered as the boundary layer thickness becomes comparable with the size of particle<sup>16,21</sup>. Significant corrections appear for particles with a density differing greatly from the surrounding liquid<sup>13,34,38</sup>. The Gor'kov potential can still be a useful approach for determining the trapping force on particles beyond the Rayleigh approximation as long as the material properties of the object are not significantly different from those of the host fluid, such as in the case of cells in aqueous solution<sup>42</sup>.

**Acoustic streaming.** Acoustic streaming is a non-linear phenomenon that arises from attenuation of an acoustic wave in or adjacent to a viscous fluid medium<sup>43</sup>. Streaming is often measured via particle image velocimetry. An important part of understanding and using streaming is its analysis, which has long been a challenge<sup>1</sup>. The approaches presented in the classic literature<sup>44–47</sup> are often difficult to apply to modern acoustofluidics because the frequencies are higher and the length scales are far smaller today, although new approaches may help<sup>48</sup>. There are also many terms unfamiliar to a new reader. Westervelt's paradox<sup>49</sup> is an example: placing a vibrating piston at one end of an open tube to cause planar acoustic waves to propagate along its length produces a zero mean mass flux and a zero Lagrangian mean of the velocity, yet the Eulerian mean of the velocity flow field is not zero and is oriented towards the piston. Stokes' drift<sup>50,51</sup> is the difference between the Eulerian and Lagrangian means of the velocity. There is the hydrodynamic Reynolds number,  $Re_{\text{hydro}} = (\rho_f u_0^2)/(\omega \mu)$ , one of several different acoustic Reynolds numbers<sup>52</sup>,  $Re_{\text{ac}} = (\beta/\alpha)[(u_1 \omega)/c_0^2]$ , and the streaming Reynolds number<sup>1</sup>,  $Re_{\text{st}} = [\rho_f (u_0 + vu_1)^2]/(\omega \mu)$ , each of which is useful in different contexts;  $u_0$  and  $u_1$  refer to the

**Rayleigh particle**

A particle that has a radius that is much smaller than the acoustic wavelength.

**Standing wave**

A stationary wave formed by the superposition of counterpropagating travelling waves, which are commonly formed by the use of opposing transducers or reflective surfaces.

**Zero mean mass flux**

The absence of mass flow.

**Zero Lagrangian mean**

The Lagrangian specification of fluid flow states that the observer follows individual fluid parcels through time.

**Eulerian mean**

The Eulerian specification of fluid flow states that the observer follows a specific location in space through which the fluid flows as time passes.

hydrodynamic and acoustic particle velocities, respectively,  $\rho_f$  is the fluid density,  $\omega$  is the angular frequency,  $\mu$  is the dynamic viscosity,  $\beta$  is the attenuation coefficient of acoustic wave in fluid, and  $\alpha$  is the attenuation coefficient of SAW or other propagating wave in substrate. The first of these Reynolds numbers is nearly ubiquitous, used in most fluid mechanics phenomena; the acoustic Reynolds number is typically used to characterize the fluid in sound propagation problems, such as noise generation; and the last is the most useful to predict flow behaviour in the presence of acoustic waves. There are also named acoustic streaming phenomena: Eckart when the longitudinal propagation of sound itself in the fluid bulk is attenuated and gives rise to flow<sup>46</sup>, Schlichting when it is driven by shear in the viscous boundary layer next to a solid surface<sup>45</sup> (sometimes referred to as microstreaming) and Rayleigh when it appears in the bulk due to coupling with Schlichting streaming<sup>44</sup>. In reality, most systems are a complex combination of these, with perhaps other phenomena thrown in<sup>53,54</sup>, making analysis and design difficult. Additionally, microscale to nanoscale fluidics is usually assumed to be incompressible, but with acoustic waves sufficient to generate acoustic forces or streaming, compressibility must be included, even when the acoustic Mach number  $u_1/c_0$  is very small, where  $c_0$  is the speed of sound and  $u_1$  is the particle (or vibration) velocity<sup>1</sup>. Even if  $u_1/c_0 = 0.001$  in water for an acoustic wave, a shock will appear 6 mm from the source.

**Combined effect on particles.** Particles in acoustofluidics generally experience acoustic radiation forces ( $F_R$ ), drag forces due to the acoustic streaming ( $F_{AS}$ ), gravity, buoyancy and other driving forces, such as external fluid flow-induced drag force<sup>55</sup>, and other field-induced forces<sup>56</sup> (for example, the dielectrophoretic force<sup>57,58</sup> or optical force<sup>59,60</sup>). These latter forces are referred to as other forces ( $F_O$ ). Thus, the total force ( $F_t$ ) exerted on the particles can be written as:

$$F_t = F_R + F_{AS} + F_O. \quad (5)$$

When these forces on the particles are balanced ( $F_t = 0$ ), the suspended particles in acoustofluidics can be trapped. With careful design, the particles may be trapped even when  $F_t \neq 0$  (REF.<sup>61</sup>). If the other driving forces vanish and the bioparticle (such as a cell, which typically has a very similar density as the suspension medium) is suspended in liquid, the gravitational and buoyancy forces have similar magnitudes but opposite directions and are almost balanced. Thus, the behaviour of particles in acoustofluidics can be characterized by  $F_R$  and  $F_{AS}$ . As  $F_R$  is proportional to the volume of the suspended particle, whereas  $F_{AS}$  scales with its radius, the former dominates for larger particles and the latter for smaller particles<sup>62–65</sup>. The critical radius  $a_c$  for which a particle's motion crosses over from being streaming-dominated (if smaller than  $a_c$ ) to radiation-dominated (if larger than  $a_c$ ) is a function of the acoustic wavelength, the intensity of the acoustic field and the viscous boundary layer<sup>65,66</sup>. For a 2 MHz standing wave parallel to a planar microchannel wall in water at room temperature, the viscous boundary layer of water is approximately 0.4 μm; the corresponding  $a_c$  of polystyrene particles has been

determined to be around 0.7 μm (REF.<sup>65</sup>). Consequently, most biological cells (with radii larger than 1 μm) are dominated by  $F_R$  and nanoscale bioparticles, such as extracellular vesicles, are dominated by  $F_{AS}$ . As a result, various acoustofluidic approaches have been developed which utilize acoustic radiation forces, acoustic streaming or their combination to manipulate target particles for a wide range of biomedical applications.

**Overview.** In this Primer, we seek to provide an overview of acoustofluidic technologies and show that although there are multiple strategies for implementing acoustofluidics in biomedical applications, they are all based on similar underlying principles. We hope to provide a unified perspective that will allow end users to choose the acoustofluidic technology that is best suited for their research needs. We have broadly categorized existing acoustofluidic technologies into two categories: bulk acoustic wave (BAW) devices and surface acoustic wave (SAW) devices. We describe the instrumentation and experimental designs used in typical acoustofluidic experiments (Experimentation), present representative examples of the data generated in conjunction with acoustofluidic devices (Results) and describe the key application areas in which acoustofluidic devices are most commonly used (Applications). We also discuss the reproducibility in the performance of acoustofluidic devices across different laboratories (Reproducibility and data deposition), review the current limitations of acoustofluidic technologies and give suggestions for optimizing device performance (Limitations and optimizations). Finally, we provide our perspective on future development of acoustofluidic technologies and potential new applications (Outlook).

## Experimentation

In this section, we provide basic information needed for two main categories of acoustofluidic experiments: BAW and SAW acoustofluidics. These two different technologies are categorized according to the acoustic wave propagating in the acoustofluidic chamber. Throughout this Primer, the term chamber refers to the fluid compartment where the liquid sample is placed. Various chamber types, including open chambers (exposed to air), closed chambers (entirely enclosed and sealed from the surrounding environment) and microfluidic channels (open or enclosed chambers with micron-sized dimensions that fluid can flow through) are utilized in acoustofluidic devices. We describe the common components and layout in both the BAW and SAW set-ups. Then, we show the specific transducers and modes used in BAW and SAW devices, respectively. Owing to the variety of implementations of acoustofluidic technologies, we focus on essential features that are shared between set-ups and point out key differences.

A standard acoustofluidic set-up includes an acoustofluidic device, a sample chamber, a function generator and a power amplifier (FIG. 1a). The acoustofluidic device generates acoustic waves to manipulate the particle and fluid in an adjacent chamber. The core component of the acoustofluidic device is the acoustic wave transducer. The transducer is usually made of piezoelectric

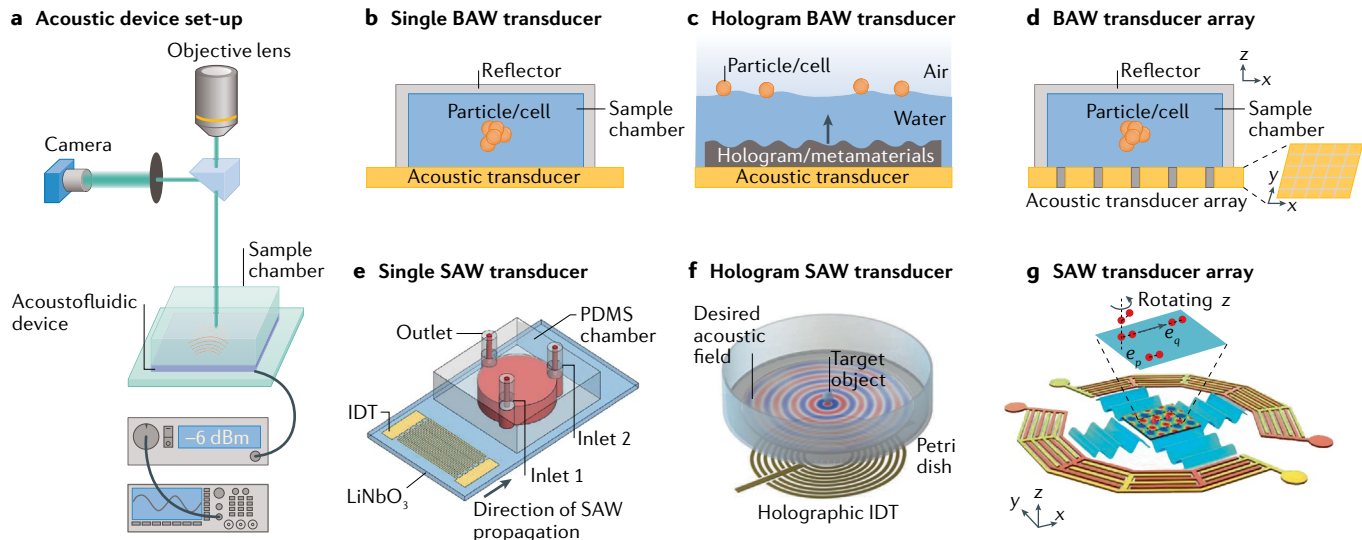


**Fig. 1 | Typical configurations of acoustofluidic devices.** **a** | Standard experimental set-up for an acoustofluidic device. A function generator and optional amplifier are connected to an acoustic transducer to generate acoustic waves. Operation of the acoustofluidic device is typically viewed through an objective lens and camera of a benchtop microscope. The acoustofluidic device can be classified as a bulk acoustic wave (BAW) device (parts **b–d**) or surface acoustic wave (SAW) device (parts **e–g**) depending on characteristics of the acoustic transducer. **b** | BAW acoustofluidic device. The standing wave is formed within the sample chamber, which can contain a single pressure node or multiple pressure nodes. **c** | Holographic BAW acoustofluidic device. The hologram placed in front of the path acoustic transmission modulates the acoustic wave to form complex, customizable pressure distributions within the sample chamber. **d** | BAW acoustofluidic device containing a multi-element array of transducers. Each element of the array can be individually addressed, enabling formation of complex,

time-varying acoustic fields. **e** | SAW acoustofluidic device employing a single pair of interdigital transducers (IDTs). SAW propagates along the surface of the substrate and can be coupled to a sample chamber (as shown) or liquid droplet to enable fluid and particle manipulation. **f** | Holographic SAW acoustofluidic device. The holographic IDT is capable of generating complex, customizable pressure distributions within a Petri dish (as shown) or sample chamber. **g** | SAW acoustofluidic device containing a multi-element array of transducers. Each transducer operates at an independent frequency, enabling formation of complex, time-varying acoustic fields. Part **e** reprinted with permission from REF.<sup>253</sup>, ACS. Parts **f** and **g** reprinted from REF.<sup>247</sup>, CC BY-NC (<https://creativecommons.org/licenses/by-nc/4.0/>).

materials, which can convert electrical signals to acoustic signals or vice versa. The excited electrical signal for the transducer is generated with a function generator and can be amplified with a power amplifier when requiring greater acoustic pressures. A microscope and camera are sometimes used to observe the manipulation of fluids and particles within the chamber. Depending on the acoustic wave generation and propagation characteristics, the transducer is categorized as a BAW transducer or SAW transducer, whereas the corresponding set-up is named BAW acoustofluidics or SAW acoustofluidics.

In practice, the acoustic transducer is a critical component. It determines the operating frequency, intensity and distribution of the acoustic field incident into the fluid chamber. The structure and acoustic properties of the chamber need to be carefully chosen, as the chamber forms an acoustic cavity, and its walls will reflect, refract or absorb the acoustic wave depending on the design. Typically, acoustofluidic devices are operated in a resonant state with a high quality factor ( $Q$  or  $Q$  factor) to minimize power consumption and produce enhanced acoustic fields<sup>67,68</sup>. The field formed inside the chamber generates acoustic radiation forces on the particles within and acoustic streaming, which drives flow within the chamber. In combination with other forces that are often of comparable magnitude — gravity, buoyancy, drag forces, van der Waals, electrostatics and so on — efficient

acoustic manipulation of the particles and liquid in the chamber can be achieved.

**BAW acoustofluidics.** A typical BAW acoustofluidic device is shown in FIG. 1b. The bulk acoustic transducer is the core component, which is often made of (hard) lead zirconate titanate (PZT) polarized ceramic plates sandwiched by metal electrodes. The polarization and electric field are typically (but not always) along the thickness direction, enabling the formation of thickness-mode vibrations at discrete resonances in the transducer. The operating frequency range of this type of PZT source is typically 20 kHz–10 MHz, and PZT does produce hysteresis<sup>69</sup>, in turn producing heating and loss intrinsic to the material<sup>70</sup> at about 0.5% of the total energy transduced in modern hard PZT materials. Above about 10 MHz, PZT tends to produce heat owing to conduction losses from elemental lead present along the grain boundaries of the ceramic material<sup>71</sup>. Single-crystal piezoelectric media, such as lithium niobate and langasite, can be used in bulk devices to expand the frequency range to 10 MHz–10 GHz or more<sup>72</sup>. The electrical characteristics of the transducer and acoustic field pattern are preferably tested before use with an impedance or network analyser. The analyser is attached to the transducer's input in place of a signal generator and amplifier to measure its resonance and anti-resonance frequencies for a given resonance mode<sup>73</sup>. Several

**Q factor**  
Shorthand for the quality factor, a parameter that quantifies the damping at each resonance frequency.

**Time-reversal principle**

A signal processing technique that can be used to focus acoustic waves to a specific location.

**Rayleigh (surface) wave**

A flexural wave isolated to a surface. Typically generated for acoustofluidics using an interdigital electrode deposited upon a piezoelectric substrate.

modes may be independently measured if they are to be used<sup>74,75</sup>. A laser Doppler vibrometer can be used to obtain the wave pattern on the surface of the transducer or chamber<sup>76</sup>. A hydrophone can be used to scan the field pattern inside the chamber<sup>77</sup>; at small scales (<1 mm), fibre optic hydrophones are useful<sup>78</sup>. Each hydrophone design has unique detection properties, with upper and lower detection limits that vary depending on where the acoustic source is with respect to the hydrophone.

The fluidic chamber is also important as its walls reflect, refract or absorb the incident acoustic waves<sup>68</sup>. Standing waves are commonly used in BAW acoustofluidics and can be formed as the result of acoustic waves reflected from the chamber wall. The acoustic properties and geometry of the chamber influence the field pattern<sup>79,80</sup>. Both acoustically hard material (such as silicon, glass and metal, whose acoustic impedance is high relative to water) and acoustically soft material (such as polydimethylsiloxane (PDMS) and polymethyl methacrylate (PMMA), whose acoustic impedance is close to water) have been used to produce the chamber through microfabrication techniques, such as etching, machining and thermal bonding<sup>68,80–82</sup>. When the chamber is formed from hard material, standing waves are ideally formed at frequencies where an integer multiple of one half the acoustic wavelength matches a given dimension of the chamber<sup>83,84</sup>. In reality, the resonance of the piezoelectric transducer and the characteristics of the fluid also influence the standing wave pattern<sup>79,85</sup>. Driven by a single acoustic source, the standing wave field pattern is defined by the geometry of the chamber for a given resonance frequency<sup>79,86,87</sup>. Alternatively, standing waves may be formed from interference between travelling waves provided by two or more acoustic sources<sup>88</sup>, and the pattern formed from it depends upon the sources' frequency, phase and amplitude<sup>89</sup>. With appropriate design, these devices can effectively pattern particles and cells, but are generally unable to provide selective trapping of individual particles.

To realize more precise particle manipulation, an effective and economical means to shape the field is adding an acoustic artificial structure (such as lenses<sup>90</sup>, holograms<sup>77</sup> and metasurfaces<sup>91</sup>) on the surface of the transducer. As shown in FIG. 1c, these artificial structures can modify the output of a single transducer to generate a high-fidelity acoustic field as desired<sup>77</sup>, providing unique features such as sub-wavelength-scale amplitude control<sup>92</sup> and complex beam patterns<sup>93,94</sup>. These shaped fields can then realize sub-wavelength particle manipulation<sup>95,96</sup> and 3D single-particle manipulation<sup>93</sup>. These artificially designed structures offer two key advantages: the simplification of the driving electronics, only requiring a single channel, and an increased phase fidelity limited only by the resolution of the machined structure<sup>97</sup>. Thus, acoustic artificial structures simplify miniaturization and integration of these devices into practical applications.

Acoustic transducer arrays have also been used to dynamically manipulate particles (FIG. 1d). The elements in these arrays are individually driven to create arbitrary and dynamically tuneable wavefronts via superposition<sup>98,99</sup>. Taking advantage of their fast update

rate, transducer array-based acoustofluidic devices can generate multiple traps via time multiplexing or quickly relocate a single trap occupied by a particle, with a velocity up to several metres per second<sup>99,100</sup>. Remarkably, a self-navigated 3D manipulation of particles in complex media has been realized based on a 256-element ultrasonic matrix array combined with a time-reversal principle<sup>98</sup>. Recently, a dynamic spatial ultrasound modulator based on digitally generated microbubbles on a complementary metal oxide-semiconductor chip surface has been proposed for dynamic manipulation of particles<sup>101</sup> while reducing the complexity of the driving system, a fascinating approach.

**SAW acoustofluidics.** A typical SAW acoustofluidic device is shown in FIG. 1e. SAW resonators convert an electrical signal provided by a signal generator and amplifier into vibration that propagates across the surface of a piezoelectric material. The speed of the Rayleigh (surface) wave is generally much less than the bulk waves that might propagate in the piezoelectric material, confining the SAW to within four or five wavelengths of the surface. This mode of propagation uses only a portion of the piezoelectric material to produce the transformation of electrical to mechanical energy, unlike BAW devices. However, the acoustic energy is confined in SAW devices such that mounting does not produce losses. When brought into contact with a fluid present on the surface, a portion of the SAW is converted to sound that propagates in the fluid<sup>102</sup>. This sound produces the acoustic pressure and streaming responsible for many of the phenomena in SAW acoustofluidics<sup>103,104</sup>. In practice, the geometry and acoustic properties of the chamber and the acoustic properties — density, speed of sound and viscosity — of the liquid loaded on the surface influence the SAW properties<sup>105</sup>. All piezoelectric materials are anisotropic, and the anisotropy is vitally important in SAW generation<sup>105</sup>: for example, in the 128YX cut of lithium niobate, the SAW is ten times weaker along the *y* axis than the *x* axis.

The SAW resonators, formed by interdigital transducers (IDTs) present on a piezoelectric substrate, are the key component of the SAW acoustofluidic instrument. The IDT is made by a set of metallic fingers connected to a common electrode — a bus bar — interdigitated with a second set of metallic fingers attached to a second bus bar, all directly deposited onto the piezoelectric layer by standard lithographic techniques<sup>106,107</sup>. The structure of the IDT determines the frequency, bandwidth and directivity of the generated SAW<sup>108</sup>. By changing the number, spacing and aperture (overlapping length) of the metallic fingers, the character of the resulting SAW can be changed<sup>103</sup>. For example, straight IDTs can generate a SAW that propagates with a laterally Gaussian distribution, focused IDTs consist of pairs of annular electrodes that can form a spatially focal point, whereas slanted-finger IDTs can vary the SAW distribution in space<sup>109</sup>. The piezoelectric layer is typically a single-crystal bulk lithium niobate substrate, langasite or a polycrystalline zinc oxide thin film deposited on a non-piezoelectric substrate (such as silicon

**Lamb wave**

A flexural wave in a structure that has a wavelength at or less than two times the thickness of the structure. Typically appears in surface acoustic wave (SAW) devices in the piezoelectric media when the resonance frequency is too low to isolate the wave to the surface.

**Pressure nodes**

Minimum pressure locations.

**Pressure antinodes**

Maximum pressure locations.

**Mie particles**

Particles of about the same size as the acoustic wavelength.

**Acoustic levitation**

The use of the acoustic radiation force to counteract gravity and suspend a particle in air.

and silicon dioxide)<sup>110</sup>. In the latter case, the substrate thickness is usually designed to be substantially larger than the SAW wavelength to avoid wave leakage and reflection through the thickness of the substrate, forcing a high frequency to be used as the lower limit to avoid energy loss into the substrate. In the past, 10–1,000 MHz has been used for SAW acoustofluidics<sup>105</sup>. However, in a vast majority of this past work, the substrate has been lithium niobate 500 μm thick; below 40 MHz the wave is not isolated to the surface and instead propagates as a bulk Lamb wave. Lamb waves are otherwise similar to SAWs, and such waves have been used for fluid manipulation, as have bulk and mixed-mode waves<sup>76,111</sup>. The laser Doppler vibrometer can be used to obtain the SAW pattern on the substrate<sup>108</sup>.

Standing SAWs are typical in acoustofluidics. Similar to BAW acoustofluidics, a pair of IDTs in opposition or an IDT and an opposing reflector can form 1D standing SAWs in the substrate, whereas two pairs of IDTs arranged orthogonally can produce 2D standing SAWs<sup>112</sup>. These standing waves can be coupled into a microfluidic chamber to enable the manipulation of liquids and particles within. Recently, more complex SAW fields have been achieved by altering the IDT shape. For example, as shown in FIG. 1f, a single spiralling IDT encodes the phase of the field similar to a hologram, which enables the generation of the targeted acoustical vortex<sup>113</sup>. FIGURE 1g shows multiple paired IDT structures evenly distributed around the coordinate origin, which are capable of dynamically reshaping SAW wave fields to provide desired pressure distributions and facilitate dynamic and programmable particle manipulation<sup>114</sup>. The anisotropy of the substrate makes arbitrary planar SAW propagation difficult without careful selection of the substrate cut<sup>115</sup>. A complex spiral IDT on an optimal 152YX cut of lithium niobate produces uniform SAWs for cell separation in blood<sup>116</sup>.

The size and physical properties of the chamber also influence the propagation and pattern of SAWs. If the fluid present on the substrate is thinner than the viscous boundary layer ( $\delta = \sqrt{2\nu_0/\omega}$ , which is about 500 nm in water with kinematic viscosity  $\nu_0 \approx 10^{-6} \text{ m}^2 \text{ s}^{-1}$  at  $f = (1/2\pi)$ ,  $\omega \approx 1 \text{ MHz}$  (REF.<sup>117</sup>)), no sound propagates into the fluid and the fluid behaves according to the propagation of the SAW<sup>118</sup>. If the fluid is thicker than this depth yet is smaller than the wavelength of sound in the fluid at the frequency of operation, sound enters the fluid to produce a 2D planar sound field<sup>119,120</sup>. When the height of the chamber is larger than the wavelength of sound in the fluid, the SAW produces a longitudinal sound wave that propagates into the bulk from the fluid–substrate interface at the Rayleigh angle<sup>102,119</sup>. Viscous attenuation of this sound produces acoustic streaming, and, depending on the attenuation length of the SAW in the substrate and the sound in the fluid<sup>121</sup>, a standing acoustic wave and fluid flow from acoustic streaming may appear in the fluid. In addition, the shape and the position of the chamber can also influence the symmetry of the field<sup>122</sup>. Similar to the BAW devices, both rigid materials (such as silicon and glass) and soft and lossy materials (such as PDMS) have been used to make the chamber in SAW devices<sup>123,124</sup>. In general, the chamber

in SAW devices tends to be smaller than BAW-based devices and fabricated using standard microfabrication techniques<sup>107</sup>.

**Results**

All variants of acoustofluidics, including BAW acoustofluidics and SAW acoustofluidics, share the common ability to manipulate particles (such as cells) and/or actuate fluid through the use of acoustic radiation forces and/or drag forces due to acoustic streaming<sup>65</sup>. In this section, we discuss some typical results from using acoustic radiation forces and acoustic streaming.

**Acoustic radiation forces.** When the acoustic radiation force is dominant in acoustofluidics, the gradient field-induced gradient force is generally responsible for acoustic trapping. For Rayleigh particles, the force potential is governed by a contrast factor that is a function of the relative density and compressibility between the particles and host fluid based on Gor'kov's formula shown in Eq. 3. Standing wave-based BAW acoustofluidics and SAW acoustofluidics have been widely used to collectively trap relatively dense and stiff particles at pressure nodes and relatively light and soft particles at pressure antinodes<sup>119,125</sup> (FIG. 2a). Note that for small heavy particles in a viscous liquid, the thermo-viscous effects can significantly influence the trapping force's amplitude and direction<sup>21</sup>. Mie particles can also be trapped at particular locations in an acoustic standing wave, but these locations cannot be determined using Gor'kov's theory and need to be specially analysed<sup>126</sup>. The Mie particles may be acoustically trapped at a pressure node, an antinode or even a midpoint between these points owing to the finite size scattering effect<sup>126–128</sup>. Recently, resonant artificial structure-induced gradient fields have been utilized to trap particles. These resonant fields are usually more localized than the standing waves, and thus can generate large gradient forces to trap smaller particles<sup>94,129</sup>. It is possible to calculate the acoustic radiation force acting on particles near a pressure node, enabling researchers to design acoustofluidic trapping devices for a range of bioparticles depending on their mechanical properties (FIG. 2b).

Selective trapping of single particles is critical in acoustofluidics. As an alternative to standing acoustic wave collective trapping, acoustic vortices have been proposed to achieve selective trapping of individual Rayleigh or Mie particles<sup>130,131</sup>. Helical waves spin around a central axis, creating a central pressure node surrounded by a ring of high pressure; particles such as cells can be trapped at the node and translated without altering their viability, enabling a highly biocompatible, contactless method for cell manipulation<sup>41,132</sup>.

Other forces also need to be considered for the 3D stable trapping of dense particles. For bioparticles in liquid, acoustic radiation forces can oppose gravity or buoyancy by increasing the acoustic power<sup>133</sup>. Particles trapped in air employ acoustic levitation; the acoustic radiation forces used in this approach need to counteract gravity and suspend objects<sup>134,135</sup>; and there is near-field<sup>136</sup> and far-field<sup>134</sup> acoustic levitation, the latter of which is more widely known but less powerful.

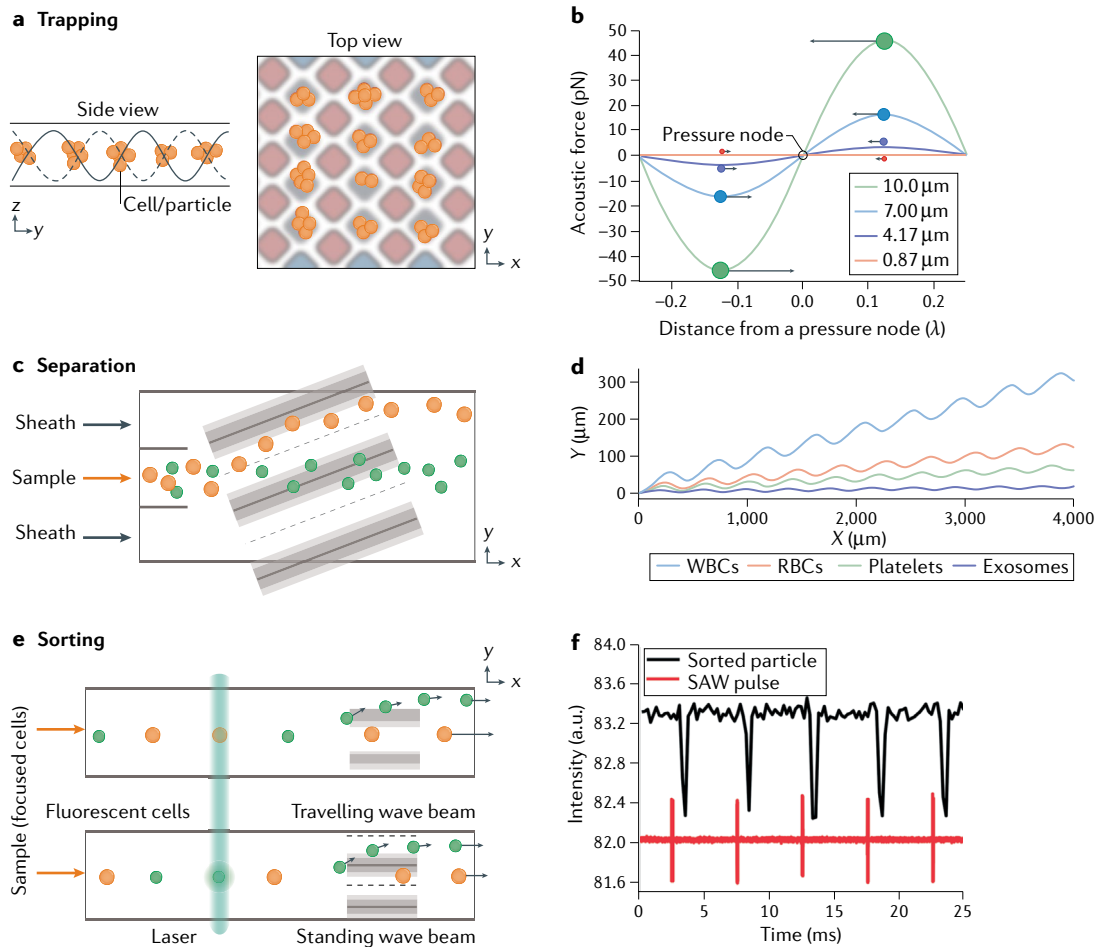


**Fig. 2 | Representative acoustofluidics results based on acoustic radiation forces.** **a** | Acoustic radiation force can be used to trap particles at pressure nodes and antinodes, depending on their mechanical properties. **b** | Acoustic radiation force distribution acting on polystyrene particles of different diameters within an acoustic wave. **c** | Acoustic radiation force-based separation of flowing particles based on differences in their physical properties. **d** | Simulation results showing trajectories of various bioparticles in a tilted-angle acoustic field. Diameter, density and compressibility of bioparticles are critical physical parameters that govern their trajectories. **e** | With integration of an optical detection unit, acoustic radiation force can be used to selectively sort particles of interest. Both standing wave and travelling wave beams have been employed for sorting of particles in continuous flow. **f** | Experimental results showing standing wave-based sorting of 10  $\mu\text{m}$  polystyrene particles. Every dip in optical intensity (black) indicates a particle passing through the sorting collection outlet. Pulse signal is also plotted (red), showing that each intensity dip exactly follows a signal pulse. RBC, red blood cell; SAW, surface acoustic wave; WBC, white blood cell; X, horizontal distance travelled along microchannel; Y, vertical migration distance. Part **b** reprinted with permission from REF.<sup>142</sup>, RSC. Part **d** reprinted with permission from REF.<sup>200</sup>, PNAS. Part **f** reprinted with permission from REF.<sup>152</sup>, RSC.

Intuitively, plane travelling wave-induced scattering forces could be responsible for transporting particles over long distances, as these forces are oriented along the net momentum's direction<sup>137</sup>. However, for Rayleigh particles, the amplitude of the force is too small to achieve particle transport<sup>40,137</sup>. Nevertheless, Mie particles have been successfully transported in the travelling SAW direction over long distances owing to the enhanced force at the resonant frequency<sup>138</sup>. Another kind of scattering force has been proposed that can pull particles towards the source, acting as a tractor beam<sup>8,139</sup>. Certain approaches have been theoretically proposed to achieve this phenomenon, such as the use of Bessel beams with a specific conic angle, such that the majority of incident momentum is scattered in the forward direction resulting in nearby objects moving backwards towards

the acoustic source<sup>8,140,141</sup>. The experimental realization of this long-range pulling force in acoustofluidics is underway.

Another method to acoustically transport particles is by using a dynamic gradient field. The dynamic standing wave can be created by using a pair of opposing transducers, so that the sum of two independent travelling waves generated by the transducers forms the standing wave<sup>142</sup>. Using such a standing wave allows the nodal positions of the field to be changed by varying the relative phase or frequency of the two transducers; thus, trapped particles can be subsequently moved<sup>143,144</sup>. Noting that, transportation can be driven over long distances by continuously adjusting the relative phase of each independent transducer<sup>145</sup>. Similarly, 2D standing wave-based transportation can also be realized by using

two pairs of orthogonal transducers<sup>143,146,147</sup>. 3D transportation can be achieved by using a dynamic acoustic hologram with a transducer array<sup>98–100</sup>. In addition, resonant-based artificial structures — for example, phononic crystals or resonant channels — can also be used to transport particles by switching the resonant frequency<sup>94,96,148</sup>.

It is possible to separate heterogeneous particle suspensions using acoustic radiation forces based on their size and material properties. This is because the acoustic radiation force is strongly dependent on the incident and scattering acoustic fields around the particle, whereas the scattering field itself depends on the particles' size, relative density and compressibility<sup>142</sup>. Combined with the liquid flow-induced drag force on particles, standing wave field-based BAW and SAW acoustofluidics have been widely used to separate particles based on their size<sup>142</sup>, density<sup>94</sup> and compressibility<sup>149</sup>. Often, owing to the different acoustic forces produced on the particles, a separation may be produced from the difference in time required for the particles to migrate to the pressure nodes or antinodes. Recently, tilted-angle standing SAWs have been proposed to separate particles (FIG. 2c). The fluid flow direction is not parallel to the standing SAW propagation, thus the maximum separation distance is not limited to a quarter of the acoustic wavelength. This configuration strongly increases the separation efficiency and sensitivity using SAW<sup>55</sup>. The physical properties of the particles and the operational parameters of the acoustofluidic device (including frequency, vibration amplitude and flow rate) can be used to simulate the trajectories of different bioparticles in the acoustic field (FIG. 2d). These simulations can be used to predict the final vertical migration distance of the bioparticles and are critical in the design of the micro-channel. An alternative approach to separate particles is using travelling waves, as the acoustic scattering force at resonant frequency can be greatly enhanced, whereas the resonant frequency is dependent on the acoustic properties of the particles<sup>138,150</sup>. In addition to continuous separation, optical detection units have been integrated with acoustofluidic devices to enable selective sorting of flowing particles<sup>151–153</sup> (FIG. 2e). In these approaches, optical feedback — such as the detection of a fluorescent signal — is used to trigger downstream transducers, which can be actuated to form a transient acoustic wave and selectively push individual cells or particles to a separate collection outlet (FIG. 2f). Both travelling wave<sup>153</sup> and standing wave<sup>151,152</sup> approaches have been implemented as the sorting mechanism for acoustofluidic particle sorting.

**Acoustic streaming.** Rayleigh SAW has long been used to collect<sup>154</sup> and concentrate<sup>122,155</sup> particles via acoustic streaming in channels at megahertz<sup>155</sup> and gigahertz<sup>156</sup> frequencies (FIG. 3a,b), in porous hydrophobic polymer media<sup>157</sup> (FIG. 3c) and in sessile droplets (FIG. 3d); there have also been observations of rare poloidal flow induced by Lamb waves for particle trapping<sup>121</sup>. Nanoparticles have also been weakly manipulated in air using SAWs, including cigarette smoke<sup>158</sup> and carbon nanotubes<sup>159</sup>. The extraction of carbon nanotubes from bundles and

subsequent patterning relies on the extreme acceleration of the piezoelectric lithium niobate substrate surface and the electric field present on the bare substrate's surface.

Acoustic streaming provides a simple means to transport particles by inducing flow in the surrounding fluid, whether within recirculation cells from an induced standing wave<sup>160</sup>, along the entire length of the channel through streaming flow and laterally through acoustic forces in a trapezoidal channel<sup>161</sup> or in racetrack designs with<sup>124</sup> and without<sup>162</sup> serpentine flow resistance. Particle transport towards concentration, sorting and separation within enclosed sessile droplets has also been accomplished, with<sup>155</sup> or without<sup>116</sup> transport of the droplet itself. Transporting particles in porous media is very difficult, especially when the pores are submicron or when the pores exist in live tissue. Acoustic streaming has been instrumental in facilitating the rapid transport of live stem cells into implantable scaffolds for tissue engineering<sup>157</sup>, the delivery of medication and functionalized particles for medical use in tissues<sup>163</sup> and the elimination of Li<sup>+</sup> ion depletion regions during the charging of lithium ion and lithium metal batteries within the separator, producing a means to enable rapidly rechargeable lithium metal batteries<sup>164</sup>. Bulk acoustic streaming from a thickness-mode device has been used to perform particle and cell separation, showing that the separation was enhanced by direct acoustic forces<sup>165</sup>.

BAW devices have also been popular for acoustic streaming; however, researchers must overcome difficulties associated with integrating bulk piezoelectric materials into the fabrication workflows for microfluidic to nanofluidic devices<sup>106</sup>. There are reports of 2.13 MHz bulk streaming in well trays used to agglomerate cells via streaming for tissue engineering and cancer trials, with methods to avoid adversely affecting the cell integrity<sup>166</sup>. A gigahertz-order bulk wave device was devised to drive acoustic streaming responsible for particle collection, alongside a method for particle image velocimetry of the streaming to even the nanoscale<sup>156</sup>. We also expect to see a growing number of applications for acoustic streaming-based particle manipulation in biomedical applications beyond the traditional trapping and transport concepts, such as work in which oocytes are denuded without contact<sup>167</sup>.

One may combine acoustic streaming with direct acoustic forces and other forces to transport and pattern particles. For example, acoustic streaming has been combined with both magnetic<sup>168</sup> forces and dielectrophoretic<sup>58</sup> forces to perform high-throughput separation of bioparticles based not only on differences in their physical properties but also on their magnetic and dielectrophoretic properties.

In sessile drops, SAWs have been used to transport, split, recombine and mix microscale droplets<sup>102,154</sup> and change their shape<sup>169,170</sup> at will, hinting at the underlying combination of streaming and acoustic radiation forces present on the fluid interface. The shear produced by streaming has been used to examine the characteristics of von Willebrand fibres responsible for clotting in blood<sup>162</sup>, and to enhance mixing at small scales for bioassays<sup>171</sup>. Generally, however, acoustic streaming is weak, producing only enough force to overcome modest

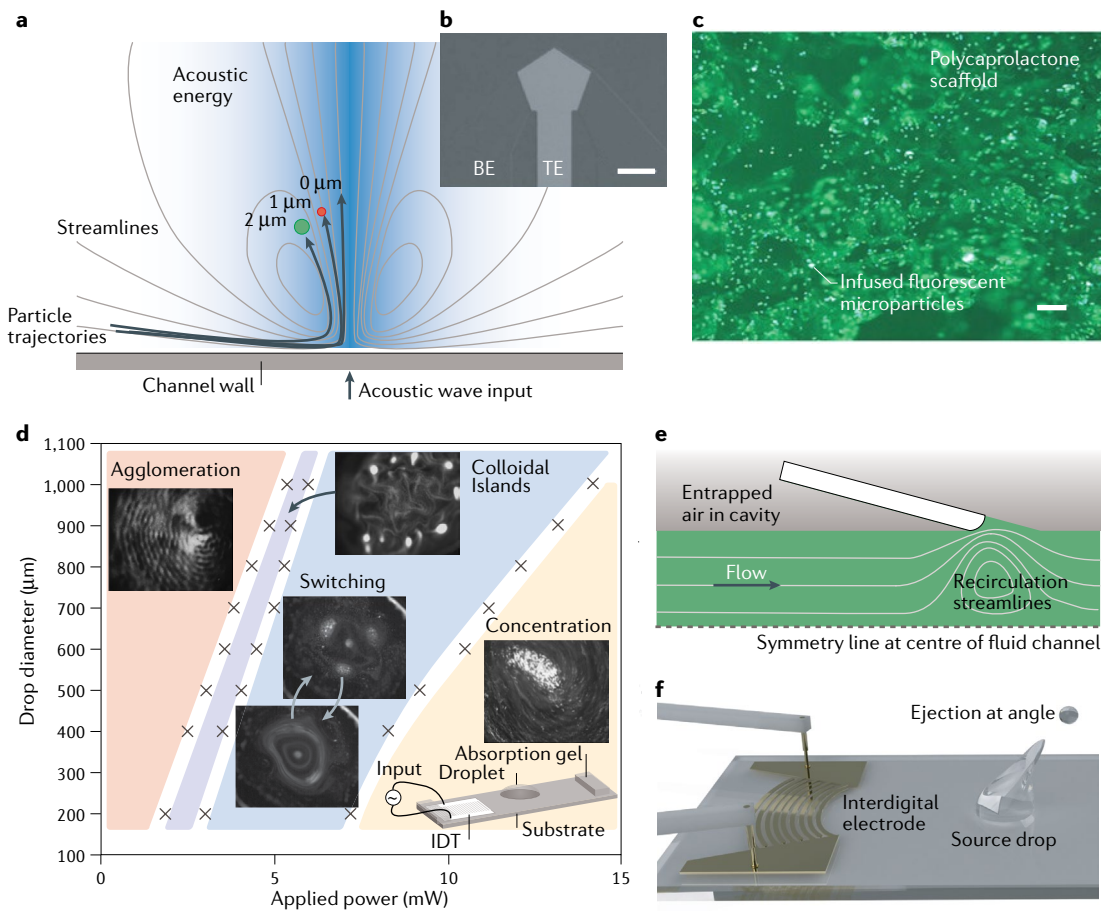


**Fig. 3 | Representative acoustofluidics results based on acoustic streaming.** **a** | Acoustic streaming may be used to segregate particles by forming regions of large shear, such as near a fluidic channel wall with an acoustic beam propagating normal to the wall. **b** | A similar approach may be used to form three-dimensional (3D) vortices, in this case using gigahertz-order ultrasound (scale bar: 200 μm). **c** | Acoustic streaming may also be used to pass particles through complex porous—even hydrophobic—media (scale bar: 100 μm). **d** | Surface acoustic wave (SAW) may be used to induce particle collection along a substrate and to form non-linear, dynamic patterning and concentration within a sessile droplet. Depending on initial size of the droplet and applied power, four distinct particle patterning regimes can be observed (each pattern type denoted by a different colour). Transition boundaries between the various particle patterning regimes indicated (x). **e** | Acoustic streaming may also be formed around encapsulated gas bubbles to pump fluids and produce particle separations. **f** | Fluids may be ejected with angular and droplet size control using SAW and thickness-mode devices via acoustic streaming and acoustic radiation pressure. BE, bottom electrode; IDT, interdigital transducer; TE, top electrode. Part **a** reprinted with permission from REF.<sup>155</sup>, ACS. Part **b** adapted from REF.<sup>156</sup>, CC BY-NC-ND (<http://creativecommons.org/licenses/by-nc-nd/4.0/>). Part **c** reprinted with permission from REF.<sup>157</sup>, Elsevier. Part **d** reprinted with permission from REF.<sup>254</sup>, APS Physics. Part **e** reprinted with permission from REF.<sup>165</sup>, RSC. Part **f** reprinted with permission from REF.<sup>54</sup>, APS Physics.

(~10 kPa) head pressures — a pressure in opposition to the desired flow — and relegating its use to racetrack designs when enclosed<sup>124,162</sup>. Some researchers have used bubbles<sup>172–176</sup> to enhance the acoustic streaming (FIG. 3e), with a small, high-shear recirculation cell designed to laterally transport and segregate particles based upon their size. This acoustic streaming method also pumps the fluid forward in the channel. Sessile drops may also simply be ejected with control over their angle and the size of the ejected droplets<sup>54</sup> (FIG. 3f). Others have used sharp structures<sup>177,178</sup>, around which the acoustic streaming flow is especially rapid. A recently discovered variation on acoustic streaming, acousto-geometric streaming<sup>53</sup>, relies instead upon the coupling between the primary acoustic field and the deformation of the channel boundary to produce fluid flow at 6 mm s<sup>-1</sup>

against even very large (>1 MPa) pressures. In nano-slit channels, this has been shown to produce rapid fluid flow and the ability to transport, split, merge, and mix 200 fL droplets of water<sup>179</sup>.

## Applications

In this section, we discuss multiple areas of research where acoustofluidic technologies have made critical advances in life science research and biomedical applications. Whereas initial demonstrations of acoustofluidic technologies were often proof-of-concept demonstrations, technological advances over the past decade have enabled acoustofluidic technologies to be actively utilized as a tool for biomedical applications. Here, we discuss the advantages of using acoustofluidic technologies to address challenges in applications ranging from

single-cell analysis to point-of-care diagnostics and provide readers with an overview of key areas of research in which acoustofluidic technologies have made a lasting impact.

**Single-cell analysis.** One of the primary applications of acoustofluidic technologies has been their integration with microfluidic platforms to provide a greater degree of control over the cellular microenvironment. For example, various acoustofluidic techniques have been developed to manipulate cells within a microfluidic chamber<sup>109,112,146,180,181</sup>, enabling researchers to control the spacing between cells, which influences both cell–cell contact processes, such as adherent junctions, as well as chemical signalling. Owing to the label-free, contactless and biocompatible nature, acoustofluidic techniques are often preferred because they do not require pre-labelling of the cells, can trap or manipulate cells over an extended duration without altering cell properties and are not reliant on the optical, magnetic or electrical properties of the cells or liquid media.

Initial demonstrations of the potential of acoustofluidic technologies to improve control over the cellular microenvironment utilized standing waves generated by BAW devices to trap microparticles and create dynamic microparticle arrays. This standing wave approach was used to develop a practical system for acoustofluidic cell trapping within a microfluidic perfusion system<sup>182</sup>. This system was capable of trapping neural stem cells and yeast cells while they were perfused by cell culture medium at a flow rate of  $1 \mu\text{l min}^{-1}$ . Furthermore, together with a contemporary study by Hultström et al.<sup>183</sup>, these studies helped establish the biocompatible nature of acoustofluidic trapping by demonstrating the viability of various cell types manipulated for up to 1 h or even more in the acoustic trap. These initial devices showed the ability to trap cells within acoustofluidic platforms and paved the way for more advanced devices for single-cell analysis.

Using orthogonal IDTs, several approaches for creating 2D arrays of trapping nodes within microfluidic chambers were demonstrated soon after. Initial implementations of these standing SAW devices demonstrated the static trapping of clusters of cells into predefined patterns within the microchannel<sup>112</sup>. Chirped IDTs — which allow for the excitation of multiple frequencies — have shown the ability to dynamically manipulate microparticles and cells within the microfluidic chamber<sup>109</sup>. The power density required for this device was 10,000,000 times less than that of optical tweezers, which contributed to its biocompatible nature. This approach was utilized to conduct cell–cell interaction studies by carefully tuning the spacing between neighbouring cells<sup>180</sup>. By applying a pulsed radio-frequency signal, cells could be pushed towards the nearest pressure node in a stepwise manner, enabling tuning of the intercellular distance (FIG. 4a). This acoustofluidic approach was used to quantitatively study contact-based intercellular communication between both homotypic and heterotypic cells by visualizing the distance-dependent transfer of fluorescent dye between cells. However, in the previously mentioned approaches for creating 2D arrays

of acoustic trapping nodes, owing to the working frequencies used (10–50 MHz), cells tend to become trapped in aggregates rather than individual cells. A key breakthrough was made by using higher working frequencies (100–230 MHz) to reduce the wavelength of the acoustic field and size of the resulting trapping nodes<sup>184</sup>. This approach enabled the generation of a 2D array with one cell per acoustic well (FIG. 4b), which was used to pattern individual red blood cells (RBCs) and lymphocytes, as well as create a convenient approach for conducting high-throughput screening of individual RBCs infected with *Plasmodium falciparum*, a parasite that causes malaria in humans. Finally, by tuning the phase angle of each individual IDT, 3D control of cells within the microchannel of standing SAW devices was demonstrated, enabling greater control over the cellular microenvironment<sup>181</sup> (FIG. 4c).

As an alternative to standing SAW approaches, focused Gaussian ultrasonic beams can also be used to trap individual cells within microfluidic chambers<sup>41</sup>. However, many of these approaches require cells to be dispersed on an acoustically transparent film, which limits its cell culture applications. In open media, when using a focused beam, cells will migrate towards pressure nodes, which limits its ability for manipulation. To overcome this limitation, several approaches utilizing acoustical vortices, or helical acoustic waves, have been developed, which enables selective trapping at the focal position of the beam<sup>130,185</sup>. However, these approaches require multiple transducers and complex electronics and are typically not flat, limiting their ability to be used in real-world applications. To circumvent these issues, precursor swirling Rayleigh waves were introduced, which can be generated by a single spiralling IDT, which then propagates through a liquid layer and can trap particles located in a microchamber above<sup>113</sup> (FIG. 4d). This design was first used to demonstrate the trapping and precise translation of  $30 \mu\text{m}$  polystyrene microparticles. Another scaled-down embodiment of acoustical vortex tweezers enabled the selective manipulation of individual cells within a microchannel<sup>116</sup>. Further improvements to the design of the acoustical vortex design enabled the selective manipulation of cells among a group of surrounding cells<sup>132</sup>, a feat that cannot be achieved using standing wave-based approaches. This platform can exert up to 200 pN on trapped cells and exhibit no impact on the short-term or long-term viability of manipulated cells. Acoustical vortex tweezers provide an excellent approach for single-cell analysis applications that require precise, selective control over the location of individual cells.

For applications requiring real-time measurements of cells' mechanical properties, the recently developed acoustic force spectroscopy platform provides a convenient acoustofluidic platform for conducting high-throughput measurements of individual cells<sup>187</sup>. Acoustic force spectroscopy requires cells to be initially confined between a glass substrate and a tethered microsphere. Using an integrated piezoelectric transducer, an acoustic standing wave may be created such that the pressure node is located above the tethered cells. When the transducer is turned on, the beads migrate towards the pressure node and pull the cell away from the substrate,

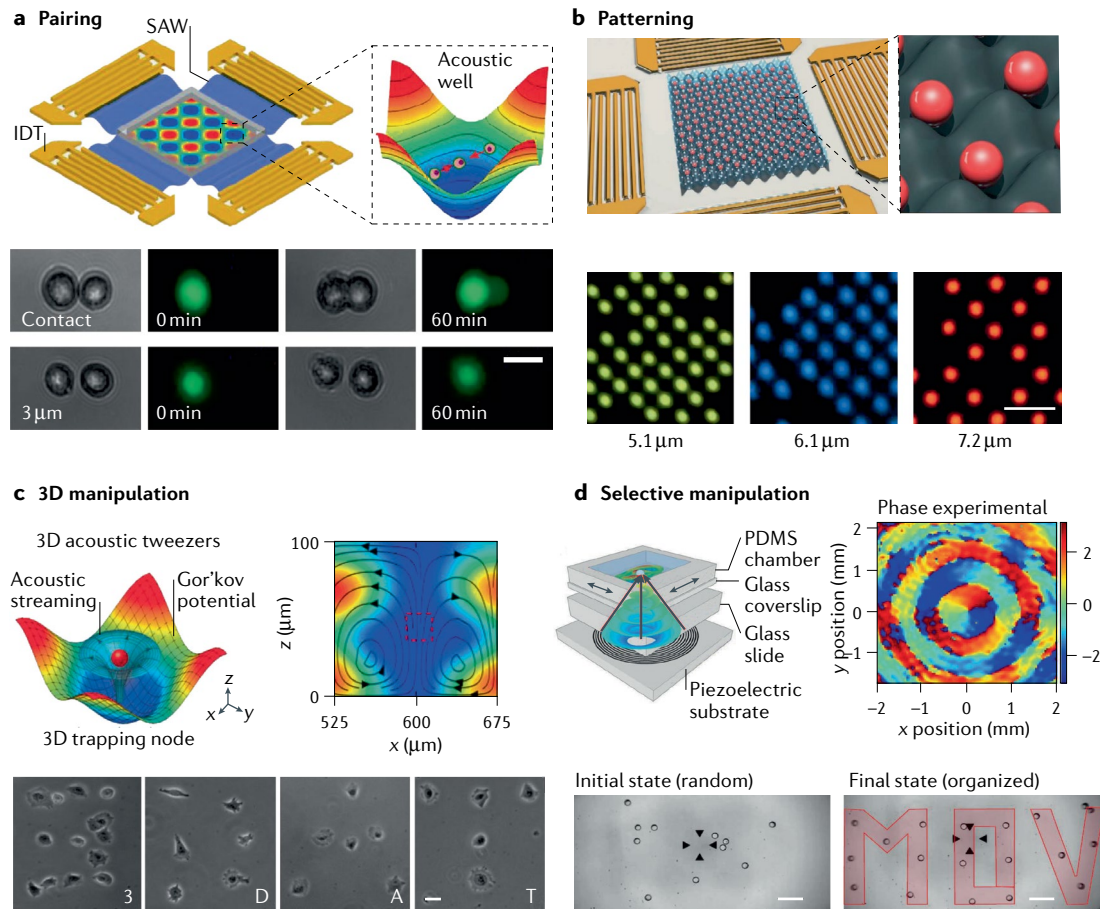


**Fig. 4 | Acoustofluidics for single-cell analysis.** **a** | Acoustofluidic device set-up can be used to pair neighbouring cells. By modulating the phase of applied acoustic waves, neighbouring cells can be brought into contact with one another, enabling detailed studies into contact-based cell–cell communication (scale bar: 20  $\mu\text{m}$ ). **b** | Standing wave acoustofluidic device for creating flexible, grid-like patterns of single cells (scale bar: 30  $\mu\text{m}$ ). **c** | Acoustofluidic device capable of manipulating trapped cells in three dimensions. By precisely controlling amplitude of applied acoustic waves, vertical position of trapped cells can be precisely controlled (scale bar: 20  $\mu\text{m}$ ). **d** | A vortex beam-based acoustofluidic device for selective manipulation of trapped cells. Unlike standing wave-based approaches, which cannot achieve selective control, use of an acoustic vortex beam enables selective trapping and manipulation of individual cells within a microchamber (scale bar: 600  $\mu\text{m}$ ). IDT, interdigital transducer; PDMS, polydimethylsiloxane; SAW, surface acoustic wave. Part **a** adapted with permission from REF.<sup>180</sup>, PNAS. Part **b** image courtesy of D. Collins and A. Neld. Part **c** adapted with permission from REF.<sup>181</sup>, PNAS. Part **d** reprinted from REF.<sup>186</sup>, CC BY 4.0 (<https://creativecommons.org/licenses/by/4.0/>).

allowing for the generation of well-controlled pulling forces up to 500 pN. Using this approach, up to 50 single cells can be measured in real time with a temporal resolution of  $\sim 1 \mu\text{s}$  (REF.<sup>188</sup>). This approach was used to investigate the effects of various chemical treatments on the mechanical properties of RBCs. The researchers applied this platform to investigate the effect of extracellular vesicles placed in the vicinity of the RBCs on their mechanical properties and showed that the presence of extracellular vesicles increased the deformability of RBCs. Subsequent demonstrations of this technology have shown its ability to measure T cell adhesion<sup>189</sup>. Through integration with an atomic force microscopy probe, more sensitive measurements of the acoustically driven vibration were made possible, enabling the measurement of supracellular mechanical properties, such as surface epithelial tension, effective viscosity and intercellular adhesive forces in a multicellular system<sup>190</sup>.

Acoustic force spectroscopy has been implemented in single-molecule analysis applications to provide a high-throughput, simple approach for measuring the force profiles of individual molecules. The configuration is similar to the configuration used to perform single-cell analysis; however, molecules, rather than cells, are tethered to the microparticle in the chamber. By creating a standing acoustic wave within the chamber, the microbead can pull the tethered molecule, exerting well-controlled forces up to 350 pN (REF.<sup>191</sup>). A transparent piezoelectric element is used, rather than an opaque element, to allow transillumination of the sample and improve the real-time tracking accuracy of the beads, and the layer thickness is optimized to allow for stronger forces along the bottom surface. This now commercialized instrument (Q-Trap; LUMICKS) has been used to measure DNA–protein binding, investigate mechanisms of DNA repair and probe the real-time

**Iso-acoustic point**

When particles or cells flow through a liquid that has a gradient in its acoustic impedance, the iso-acoustic point represents the location where the acoustic contrast between the particle/cell and the surrounding liquid is zero.

**Exosomes**

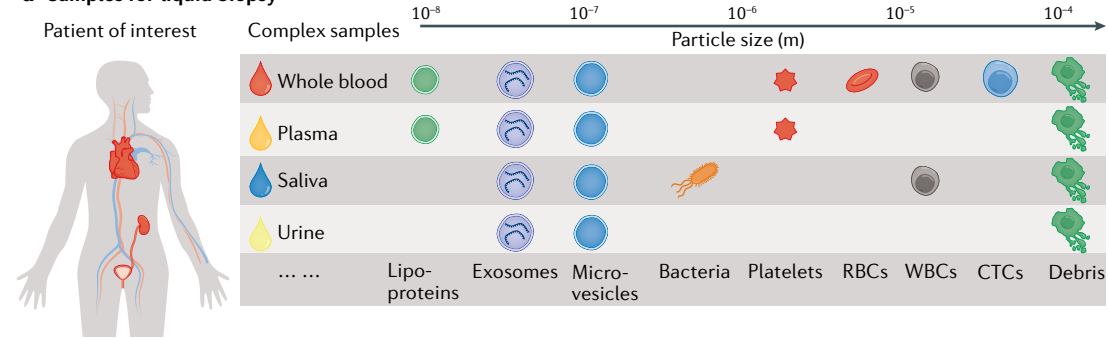
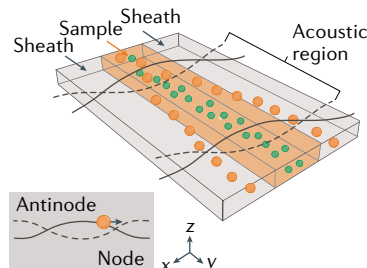
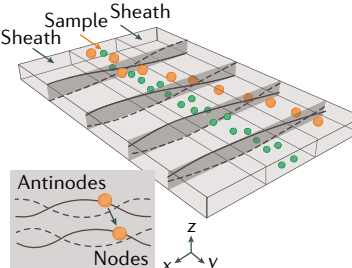
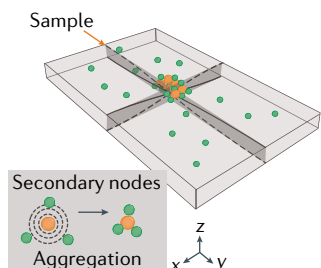
Nanometre-sized extracellular vesicles that contain molecular cargo from their cell of origin.

formation of viruses. Owing to its simple device set-up and high-throughput nature, acoustic force spectroscopy can greatly expand the use of single-molecule techniques in life science research and provide a more rapid approach for conducting large-scale measurements of individual cells or molecules.

To circumvent the need for sample preparation in acoustic force spectroscopy, several label-free, continuous-flow acoustofluidic technologies have also been developed for measuring the mechanical properties of cells and model organisms. For example, a BAW resonator was used to measure the acoustic properties and phenotypic information of cells in a manner that is independent of cell size<sup>149</sup>. By flowing cells through a BAW resonator that contained a medium with a gradient in its acoustic contrast, cells could be pushed to an iso-acoustic point. Based on the location of the iso-acoustic point of a particular type of cell, its acoustic impedance can be extrapolated and measured. This tool enables researchers to measure phenotypic information about cells in a manner that is independent of their size. BAW resonators have also been used to measure the compressibility of model organisms such

as *Caenorhabditis elegans*<sup>192</sup>. By tracking the trajectory of the *C. elegans* towards the nodal line, the compressibility of the worm can be measured. This biocompatible acoustofluidic platform holds promise for measuring the compressibility of other non-spherical biological model organisms and pathogens.

**Diagnostics and liquid biopsies.** The isolation of circulating biomarkers from biofluids is critical to the development of highly sensitive diagnostic techniques<sup>193</sup> (FIG. 5a). For example, in cancer diagnostics, the isolation of circulating tumour cells (CTCs) from whole blood has been identified as a non-invasive approach for the detection of early-stage cancers<sup>194</sup>. Similarly, exosomes have been identified in biofluids as promising circulating biomarkers for the diagnosis of cancers, neurodegenerative diseases, liver disease and gastrointestinal diseases<sup>195</sup>. However, challenges associated with the isolation of these circulating biomarkers have thus far prevented their widespread clinical use and, in many cases, the promise of developing non-invasive liquid biopsies remains elusive. Owing to their ability to separate particles based on differences in multiple physical properties,

**a Samples for liquid biopsy****b Coaxial separation****c Tilted-angle separation****d Seed bead-assisted separation**

**Fig. 5 | Acoustofluidics for point-of-care diagnostics.** **a** | Acoustofluidic devices are capable of isolating various bioparticles ranging across the nanometre to micrometre length scale from diverse biofluids, including whole blood, plasma, saliva, urine and cell culture media. **b** | Isolating bioparticles using a half-wave resonator. Particles can be separated to either pressure nodes or antinodes based on differences in their physical properties (size, density and compressibility) and collected from separate outlets and the end of the microchannel. **c** | Isolating bioparticles using a tilted-angle approach. Particles can be pushed across multiple pressure nodes, enabling larger separation distances between particles with minute differences in their physical properties. **d** | Seeding-particle-based approach for isolating bioparticles. Micron-sized particles are preloaded into the microchannel. As bioparticles are introduced, secondary radiation forces between the bioparticles and the seed particles enable selective trapping of particles of interest. Subsequent elution or washing allows the particles to be collected with high purity. CTC, circulating tumour cell; RBC, red blood cell; WBC, white blood cell. Part **b** adapted with permission from REF.<sup>199</sup>, ACS. Part **c** adapted with permission from REF.<sup>200</sup>, PNAS. Part **d** adapted with permission from REF.<sup>205</sup>, ACS.

including size, density and compressibility, acoustofluidic techniques have shown great promise in isolating circulating biomarkers and represent a powerful toolset in helping unlock the clinical utility of the liquid biopsy.

Numerous approaches have been developed for the isolation of CTCs using acoustofluidics. One of the first proof-of-principle devices was demonstrated for isolating rare cancer cells using a bulk acoustic standing wave device (FIG. 5b) to separate prostate cancer cells from white blood cells (WBCs) based primarily on differences in their size<sup>196</sup>. Under this configuration, the larger cancer cells experience a larger acoustic radiation force and are pushed to the centre outlet of the channel, aligning with the pressure node, whereas the smaller cancer cells do not experience enough force and remain in the side outlets. Cancer cell recovery ranged from 72.5% to 93.9% whereas the purity ranged from 79.6% to 99.7% at a throughput of  $70 \mu\text{l min}^{-1}$ . As an alternative acoustofluidic technique for isolating CTCs, a tilted-angle standing SAW device was employed to separate CTCs from peripheral WBCs<sup>197</sup>. Unlike traditional standing SAW devices, which can only move cells or bioparticles a distance that is equal to a quarter of the wavelength of the acoustic waves, the tilted-angle design enabled cells and particles to travel across multiple nodal lines, leading to separation distances approximately three times larger than the acoustic wavelength (FIG. 5c). As a result, CTCs could be separated from WBCs at a flow rate of  $20 \mu\text{l min}^{-1}$ , with recovery rates ranging from 83% to 96% and a WBC removal rate of approximately 90%. Later, this tilted-angle design was improved upon through the use of a PDMS–glass hybrid channel, which led to increased acoustic energy within the channel and enabled CTCs to be isolated at throughputs of  $125 \mu\text{l min}^{-1}$  (REF. <sup>198</sup>).

In addition to separating CTCs at the microscale, acoustofluidic separation technologies have been implemented at the nanoscale to separate exosomes, which range in diameter from 30 to 150 nm, from various biofluids. Owing to their small size, traditional methods for isolating exosomes, such as ultracentrifugation, suffer from drawbacks such as lengthy processing times, low yields, low purities and low biocompatibility. Acoustofluidic technologies present an opportunity to isolate exosomes in a point-of-care fashion in as little as 10 min. One of the first demonstrations of acoustofluidic technologies to filter extracellular vesicles was the use of a standing SAW design to purify nanoscale vesicles ( $<200 \text{ nm}$ ) from cell culture media<sup>199</sup>. Later, a tilted-angle SAW device was implemented to isolate exosomes from whole blood, removing  $>99.999\%$  of blood cells<sup>200</sup>. This acoustofluidic platform was later implemented to isolate exosomes from whole blood to assess their utility as a biomarker for traumatic brain injury<sup>201</sup>. An optimized design was also used to isolate exosomes from saliva<sup>202</sup>. The acoustofluidic platform exhibited a yield of exosomal small RNA that was 15 times greater than traditional ultracentrifugation. In addition to SAW-based approaches, seed particle-enabled acoustic trapping has also been used for isolating exosomes from biofluids<sup>203–206</sup>. In these devices, preloaded seed microparticles are placed into an acoustic standing

wave; as nanoparticles pass through the active acoustic region, scattered sound interaction enables them to be trapped within the microchannel (FIG. 5d). This technique typically allows for higher throughput than purely SAW-based mechanisms; however, seed microparticles are included in the isolated preparations. The protein content of extracellular vesicles isolated via acoustic trapping has been shown to be similar to extracellular vesicles isolated via ultracentrifugation. Furthermore, vesicles can be isolated directly from cell culture conditioned media, urine and blood plasma samples at flow rates of  $15 \mu\text{l min}^{-1}$ , demonstrating the powerful potential of this platform in liquid biopsy applications<sup>205</sup>.

**Automation.** Many procedures in life science research laboratories, such as the pipetting of liquids and the formulation of buffers and reagents, are manual processes that require trained technicians and are prone to operator error. One of the primary applications of acoustofluidic devices has been the automation of workflows in biological and biomedical laboratories. For example, the recently developed platform known as digital acoustofluidics is a contact-free liquid handling technology that enables the manipulation of liquid droplets with volumes from 1 nl to  $100 \mu\text{l}$  along any planar axis via acoustic streaming-induced hydrodynamic traps<sup>207</sup> (FIG. 6a). These droplets, which float on top of a layer of oil, are not prone to cross-contamination as is the case for traditional dielectrophoretic-based droplet handling mechanisms and can be merged, split and translated along any arbitrary path within the device. In addition to automated liquid handling, various acoustofluidic devices have been developed to automate the selection and sorting of cell populations. Both SAW<sup>151,208</sup> devices and BAW<sup>209</sup> devices have demonstrated the ability to sort cell populations based on detection of target fluorescence signals (FIG. 6b). These strategies have also been adopted to enable the sorting of model organisms, such as *C. elegans*<sup>210</sup>. Another key function of acoustofluidic devices has been their ability to mix fluids within microfluidic devices (FIG. 6c). Owing to the small channel dimensions and resulting low Reynolds numbers, fluid flow within microfluidic channels is often laminar, making it difficult to effectively mix fluids<sup>211</sup>. Various acoustofluidic approaches, including oscillating structures<sup>177</sup>, oscillating microbubbles<sup>212</sup> and induced fluid streaming<sup>213</sup>, have been implemented to controllably mix fluids within microfluidic devices. Acoustofluidics can also provide a high degree of automation in the concentration of analytes within small fluid volumes<sup>214–216</sup> (FIG. 6d). SAW-based<sup>214,215</sup> and BAW-based<sup>216</sup> streaming have been used to concentrate nanometre-sized particles for signal enhancement and analyte enrichment.

**3D culture and tissue engineering.** Acoustofluidics has increasingly been applied to the field of tissue engineering to pattern cells and assemble organoids for fundamental biological research<sup>217</sup>. Initially, these devices utilized standing acoustic waves to agglomerate cells and form size-controllable organoid structures<sup>218</sup> (FIG. 7). By coating a multiwell plate with a protein-repellent amphiphilic polymer coating and mounting it to a BAW

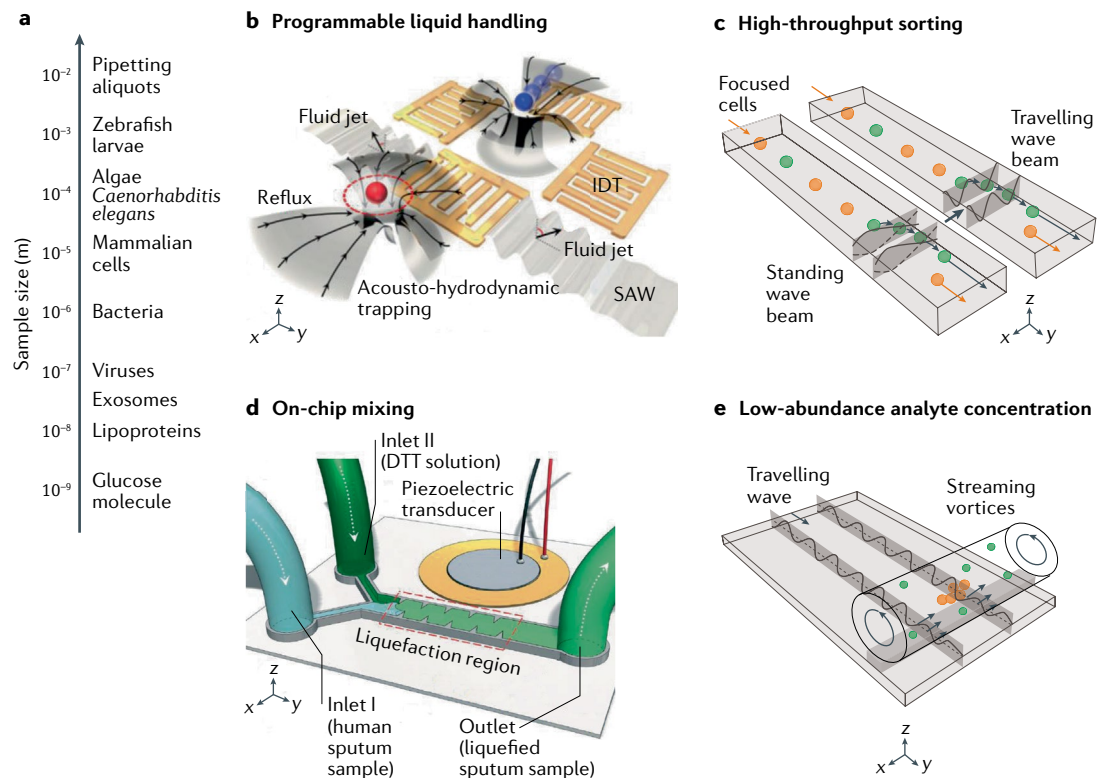


**Fig. 6 | Acoustofluidics for the automation of workflows in biomedical laboratories.** **a** | Scale bar showing the size range of common objects that are handled by acoustofluidic devices in biomedical laboratories. **b** | Acoustic streaming-based approach for manipulating liquid droplets in a contact-free manner. **c** | Acoustofluidic approaches for high-throughput cell sorting. Focused cells can be deflected from their focused streamline into a separate collection outlet through application of either standing waves or pulsed travelling waves. **d** | Acoustofluidic fluid mixing. One approach for mixing fluids via acoustofluidics involves use of sharp-edge structures embedded within the microchannel walls, which when actuated by a piezoelectric transducer oscillate rapidly and produce streaming patterns that rapidly and controllably mix fluid reagents. **e** | Acoustofluidics for analyte concentration. By applying a travelling wave to a capillary, well-defined acoustic streaming patterns can be generated within the capillary, which can be exploited to concentrate low-abundance, nanometre-sized analytes into the centre of the capillary. IDT, interdigital transducer; SAW, surface acoustic wave. Part **b** reprinted from REF.<sup>207</sup>, CC BY 4.0 (<https://creativecommons.org/licenses/by/4.0/>). Part **d** adapted with permission from REF.<sup>255</sup>, RSC. Part **e** reprinted with permission from REF.<sup>61</sup>, ACS.

transducer to create a standing wave within each chamber, highly homogeneous multicellular tumour spheroids were generated at the centre of 100 microwells<sup>218</sup>. A high-throughput, SAW-based approach was implemented for the generation of tumour spheroids<sup>219</sup>. A standing SAW with 12,000 pressure nodes was formed underneath a PDMS microchannel with 60 parallel channels; when the acoustic waves were turned on, cells in the channel aggregated at each of the pressure nodes, enabling the rapid formation of ~12,000 spheroids per chamber. In addition to the generation of spheroids, acoustofluidic devices can be used for the formation of patterned cell fibres. Both BAW<sup>220</sup> and SAW<sup>221</sup> approaches have been implemented to pattern cells within a hydrogel using a standing acoustic wave. Upon curing of the hydrogel, fibrous cellular structures that resemble natural tissue structures, such as anisotropic muscle tissue<sup>220</sup>, have been demonstrated. A hybrid SAW and BAW approach has been used to create more complex, functional collateral cylindroids for ischaemia therapy<sup>222</sup>. A PDMS chamber containing cells in a hydrogel was placed on top of a SAW substrate and acoustic coupling layer; a standing SAW was created within the coupling layer, which

was transmitted to the PDMS chamber in the form of a BAW. The reflection of the BAW from the top cover glass on the chamber enabled the formation of a 3D acoustic field to pattern multiple cell types. Although this approach enabled the fabrication of 3D structures, the patterns that could be generated were still limited to periodical structures owing to the nature of the standing waves. Newly developed acoustofluidic technologies, such as the integration of acoustic holograms, have been developed for the formation of arbitrary, complex cell patterns within hydrogels<sup>100,223,224</sup>. Here, acoustic holograms are used to create complex streaming patterns within the hydrogel, which can be utilized to bring cells to the image place and form arbitrary, predefined shapes and patterns. Holographic approaches hold great promise for the fabrication of biomimetic tissues, which require non-symmetrically shaped cell assemblies.

#### Reproducibility and data deposition

Although it is relatively straightforward to set up and operate an acoustofluidic system, reproducing data is still a challenge. Many acoustofluidic systems are designed for producing 1D acoustic fields inside

microscaled fluid channels. However, suppressing effects from resonances in the other dimensions is difficult and must be taken into consideration<sup>225</sup>. For this reason, even repeating experiments in the same system is a challenge; for example, if a BAW-type piezoelectric transducer is positioned or aligned differently onto a microfluidic chip between different experiments, or if the droplet volume changes in a droplet-based SAW system. One simple strategy to improve robustness and, in turn, data reproducibility is to design acoustofluidic devices that are as simple as possible<sup>67</sup>. On the other hand, advanced life science applications may demand complex designs and devices. Therefore, when modelling and designing a robust acoustofluidic device in general, it is recommended to include a full-system approach including all materials and three dimensions as well as the piezoelectric transducer<sup>226</sup>. But it can also be important to study individual parts of the system, for example, when selecting the thickness and material of the coupling layer between a transducer and a microfluidic device<sup>227</sup>, a minor yet important detail that is often omitted both in the design process and in practical laboratory work. Of particular interest for future BAW-based designs is thin-film BAW technology, which has the potential to significantly improve reproducibility because, unlike traditional BAW devices, the performance of the device is not reliant on the resonance properties of the transducer itself<sup>228</sup>.

In the early days of acoustofluidics, manual calibration was often needed before starting any experiment; for example, by manually fine-tuning the actuation frequency and voltage until finding a suitable resonance frequency and particle manipulation effect. Later, semi-automated procedures for selecting an optimal actuation frequency have been demonstrated, including automatic frequency tracking<sup>229</sup> and frequency modulation<sup>144</sup> methods. More recently, efforts have been made in using polymer materials as a replacement for the traditional supporting structures around a fluid channel made in hard materials such as silicon and glass. To get a polymer-based acoustofluidic system to work properly, careful modelling of acoustic resonances in three dimensions and in the whole system is needed in the design procedure<sup>230</sup>. Here, an interesting option is to exploit asymmetrical architecture and actuation for improved performance in both polymer devices<sup>80</sup> as well as traditional glass–silicon devices<sup>231</sup>. But for any choice of system design, it is crucial to know the acoustical and mechanical properties of all materials used in the device, including the sample being manipulated. Often, material properties are either unknown or not accurately quantified, and sometimes depending on external parameters that may vary during an experiment. This is particularly true in biomedical applications using complex fluid samples containing bioparticles and various chemicals. Furthermore, cells typically have heterogeneous

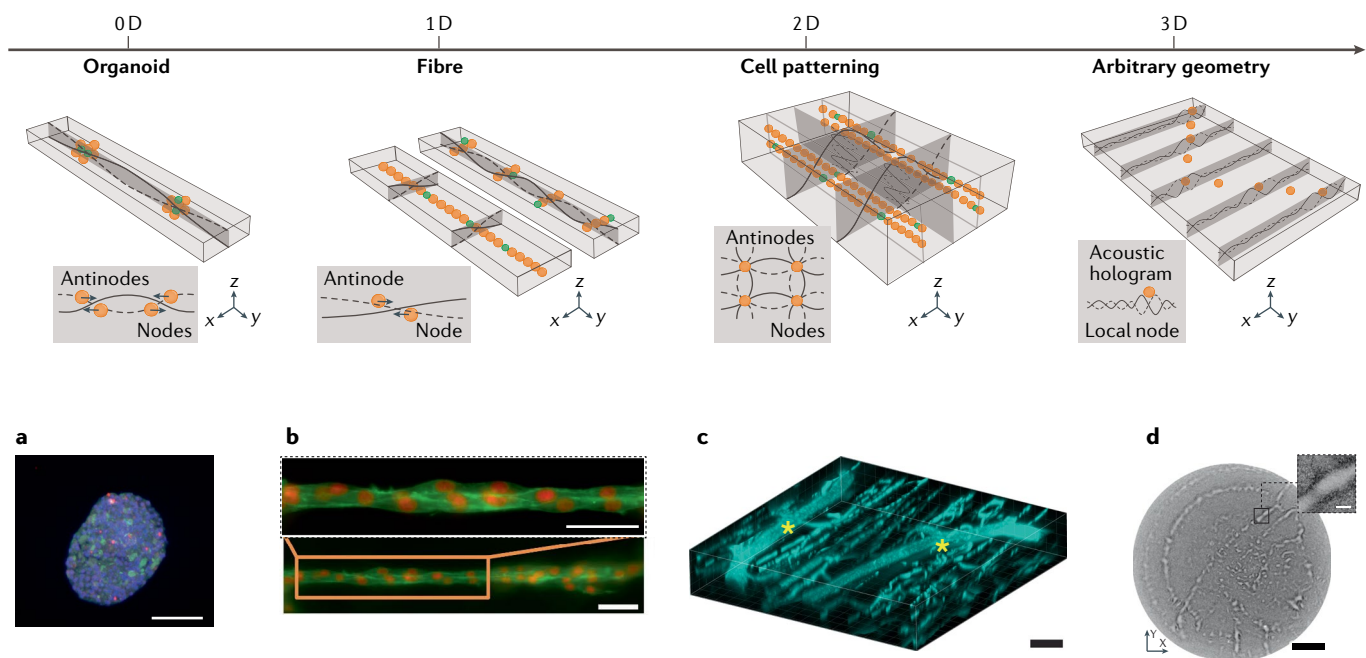


**Fig. 7 | Acoustofluidics for tissue engineering.** **a** | Acoustic standing waves can be used to rapidly form size-controllable cell clusters, representing a simple approach for the fabrication of cell spheroids and organoids (scale bar: 20 µm). **b** | Standing waves can also be used to pattern cells and form one-dimensional (1D) tissue fibres (scale bars: 50 µm). **c** | Orthogonal standing waves can be used to pattern cells in two dimensions, enabling fabrication of complex cellular geometries that incorporate multiple cell types. Here, patterned cell–hydrogel constructs were transplanted into living mice. This 3D image of fluorescently labelled blood vessels was taken 1 week after

transplantation. The yellow asterisks indicate host blood vessels that had infiltrated into the transplant (scale bar: 50 µm). **d** | Acoustic holograms have been used to create arbitrarily shaped acoustic fields, which can be used to trap cells in complex geometries that are required for formation of biomimetic tissue structures (scale bar: 5 mm; inset scale bar: 500 µm). Part **a** reprinted with permission from REF.<sup>256</sup>, RSC. Part **b** reprinted from REF.<sup>247</sup>, CC BY-NC (<https://creativecommons.org/licenses/by-nc/4.0/>). Part **c** reprinted from REF.<sup>222</sup>, CC BY 4.0 (<https://creativecommons.org/licenses/by/4.0/>). Part **d** reprinted from REF.<sup>224</sup>, CC BY 4.0 (<https://creativecommons.org/licenses/by/4.0/>).

mechanical properties within a cell population<sup>149</sup>, and these properties also depend on the cellular state<sup>232</sup>. Another challenge is to predict the acoustic effects of various concentrations of cells, particles and chemicals in a fluid sample<sup>233</sup>.

A possible route for improving the reproducibility in acoustofluidics is to integrate the piezoelectric transducer in the device, instead of having the transducer and the device as separate units. In many cases it is convenient to be able to disassemble the device, but this often comes at the cost of robustness. For example, a simple and robust device was recently demonstrated where the manipulation principle was based on surface displacement of resonance modes in the piezoelectric layer that was coupled into the fluid layer in direct contact with the piezoelectric layer. With this device, the particle manipulation function was not even affected by the introduction of a large gas pocket into the fluid sample, because the manipulation principle was not based on lateral resonances in the fluid chamber but, rather, the bulk modes of the transducer<sup>234</sup>.

In the acoustofluidic community, there are no established standards or routines for deposition of data sets and other additional information of interest. Typically, information regarding the operating frequency (kilohertz to gigahertz), operating power (1–500 mW), duration of applied acoustic waves (seconds to minutes) and throughput ( $1\text{ nl min}^{-1}$ – $100\text{ ml min}^{-1}$ ) is reported in acoustofluidics publications; however, a lack of standardization has contributed to difficulties when trying to compare results between different acoustofluidic technologies. Although this is well established in some fields, such as in proteomics and genomics, it is up to the community to agree on what type of raw data and algorithms used should be openly available for validation and further analysis. One recommendation is to include detailed experimental protocols (see Supplementary Box 1) and upload programming code, algorithms and data sets of interest to a cloud-based repository. Transducer characterization data, for example electrical impedance spectra, to facilitate more detailed evaluations and comparisons of different types of transducers and their operating frequencies should also be included. The electrical impedance spectra of a transducer can be obtained using commercially available network analysers.

### Limitations and optimizations

It is important to optimize the actuation frequency and voltage, as well as selecting proper geometries and material properties in the modelling process of the device. It is also important to choose which parameters should be prioritized in the optimization — for example, whether the power consumption or manipulation flexibility is the most important factor. Minimizing power consumption is typically done by maximizing the quality factor of the acoustic resonance<sup>67</sup>. On the other hand, this leads to limitations in frequency choice and, in turn, versatility and flexibility of the acoustic manipulation. In lower quality factor devices, several resonance modes in a fluid channel — in different directions — can be excited simultaneously with a single frequency, given that their resonance frequency spectra overlap. For example,

orthogonal resonances can be simultaneously excited in a microchannel with a square-shaped cross section to enable 2D acoustic focusing of sub-micrometre particles<sup>235</sup>. Another interesting approach is to use thin-film BAW transducers in acoustofluidics, with the advantage of being able to build devices that are insensitive to the Q factor and resonance properties of the transducer<sup>228</sup>.

It is also possible to excite acoustofluidic systems with dynamic and/or multiple frequencies. Depending on the rate of frequency change, the result is either a resonance built up from the average of the single frequency resonances or a dynamically varying resonance. The former method — fast frequency modulation — has been used for stabilizing resonances and suppressing spurious modes<sup>144</sup>, fine-tuning the pressure node position in a microchannel by rapid mode switching<sup>236</sup> and improving the roundness and uniformity of spheroids in 3D cell cultures<sup>218</sup>. The latter method — slow frequency modulation — has been used for flow-free transport of particles in a fluid channel<sup>144</sup> and for stimulating a cell aggregate by oscillatory fluid shear stresses<sup>237</sup>. These actuation strategies can be combined with frequency tracking methods where the electrical impedance spectrum is continuously monitored during actuation, which makes it possible to dynamically optimize the actuation frequency<sup>229</sup>. This is particularly important for robust long-term operation.

As briefly mentioned in the previous section, acoustic streaming causes a limitation in how small objects can be efficiently manipulated by acoustofluidic methods. Several methods have been suggested and demonstrated for reducing the influence of acoustic streaming on the manipulation performance of particles in the sub-micrometre regime. Examples include the use of larger seed particles that attract sub-micrometre particles by acoustic interaction forces<sup>203</sup>, the use of 2D acoustophoresis in channels with square cross sections, suppressing acoustic streaming by shape-optimized channels<sup>238</sup> and suppressing acoustic streaming using acoustic impedance gradients<sup>239,240</sup>. There is also the opportunity to explore the constraint of fluid volumes by the use of extremely small enclosed fluidic channels and other forms of acoustically driven flow besides acoustic streaming<sup>53</sup>.

In biomedical applications, temperature effects are important to control. High Q factor devices are advantageous as they typically produce very little heat. On the other hand, low and medium Q factor devices may produce significant heat that needs to be controlled. This is particularly true for devices including layers of polymers, PDMS, glue and other acoustically lossy materials. Even if a temperature increase is not a problem from an application point of view, it is still important to control the temperature as it affects the sound velocity and, in turn, the resonance condition. Various heat management methods in acoustofluidics have been presented<sup>241–243</sup>, including the indirect frequency tracking method<sup>229</sup>.

A question that is often asked is whether acoustic manipulation and trapping is harmful to biological cells. There are two obvious ways to harm cells by

**Acoustic cavitation**

The growth and collapse of microbubbles under the influence of an acoustic field in liquids.

ultrasound acoustics: either by heat caused by ultrasound or by acoustic cavitation. Heat can indeed be generated in any acoustofluidic device, but heat can also be limited and controlled in various ways as discussed above. Cavitation, on the other hand, is more difficult to both measure and control, but is rarely present at the frequencies and energy densities used in most acoustofluidic systems<sup>244,245</sup>. In addition, in standing wave-based acoustofluidic devices, even if cavitation should be present cells are physically protected from the cavitation bubbles as cells are typically driven to pressure nodes whereas cavitation bubbles are typically formed in pressure antinodes<sup>246</sup>. Finally, it should be noted that in acoustofluidic cell handling devices, acoustic streaming rarely has magnitudes capable of creating cell damage due to shear stresses. For example, acoustic streaming velocities were  $120 \mu\text{m s}^{-1}$  at maximum in a 2.5 MHz standing wave acoustic field with 1 MPa pressure amplitude, without causing any observable cell damage or stress<sup>242</sup>.

**Outlook**

Much progress has been made in the development of acoustofluidic technologies over the past decade. Acoustofluidic devices are now being employed in many application areas including single-cell analysis, laboratory automation, point-of-care diagnostics, 3D cell culture, tissue engineering, cell and gene therapy, biophysical measurements, drug delivery and biosensing. Although these application areas are extensive and diverse, there are still many challenges in the development of acoustofluidic technologies that need to be addressed in order to unlock the full potential of acoustofluidics in biomedical applications.

One of the primary obstacles preventing the widespread use of acoustofluidic technologies in biomedical applications has been a lack of focus placed on prototype development. The acoustofluidic technologies that have been developed thus far have largely been specialized instruments that require highly skilled operators. This has made it difficult to translate the use of acoustofluidic technologies outside specialized laboratories. Furthermore, demonstration of acoustofluidic capabilities often requires the use of external equipment, such as syringe pumps, function generators and amplifiers, which are not available to many biomedical research laboratories. Over the next decade, it is critically important for acoustofluidic technologies to be developed into all-in-one prototypes that do not require external equipment or a high degree of user skill or training. Although recent efforts have led to the commercialization of some acoustofluidic technologies — such as the z-Movi by LUMICKS for performing acoustic force spectroscopy measurements, the ekko technology platform by FloDesign Sonics for the processing of cells in cell and gene therapy manufacturing and the Attune Flow Cytometers by Thermo Fisher Scientific that acoustically focus cells prior to analysis — commercial development is still in its infancy. The current state of acoustofluidics research is in many ways analogous to the early development of commercial 3D printing technologies, where initial research efforts were conducted

by various, specialized laboratories focusing on different approaches. Another avenue that will lead to the rapid adoption of acoustofluidic technologies is the integration with existing tools for biomedical research laboratories, such as the recent demonstration of acoustic tweezers that operate within Petri dishes<sup>247</sup>. Additionally, recent development efforts have focused on open source development<sup>248</sup>, which has made acoustofluidic technologies more widely accessible to biomedical research laboratories. Overall, now that many of the key functionalities of acoustofluidic technologies have been successfully demonstrated, we expect that commercialization efforts and prototype development will rapidly follow in the coming decade.

Another key challenge in acoustofluidic research has been a lack of standardized methods to characterize the influence of acoustic waves on cells and organisms. Although multiple laboratories have demonstrated the broad biocompatibility of acoustofluidic technologies on cells<sup>242,249,250</sup> and organisms<sup>251</sup>, these evaluations have been highly specialized, making it difficult for biomedical researchers to know *a priori* the influence of a given acoustofluidic technology on their cell or organism of interest. As such, a larger focus needs to be placed on standardizing the characterization of the biological effects of acoustics at specific frequencies and powers in order to assure biomedical researchers that the technology is compatible with their research goals.

There are several challenges for the future in acoustofluidics in terms of optimizing devices and methods. One challenge is to increase the level of automation and, in turn, robustness in acoustofluidics. This can be accomplished by more advanced actuation methods including tailored frequency modulation and frequency tracking methods, but also by whole system modelling when designing new devices. It is also important to combine and integrate acoustofluidic technology with other methods such as sensor and analysis technologies. Another challenge is to improve methods for nanoparticle manipulation for handling of bacteria, viruses and exosomes. This can be explored by various suggested methods<sup>203,235,239,240</sup>, where some ideas are still only presented theoretically or numerically<sup>238</sup>. Heat management methods need further attention<sup>243</sup>, as well as additional studies of acoustic streaming in three dimensions and in various fluids, geometries and frequency regimes. New device materials should be further explored, including polymer-based materials and, possibly, hybrid materials with tailored acoustic properties. Here, asymmetrical architecture and actuation strategies have shown great promise. Novel transducer technologies applied to acoustofluidics are interesting, such as thin-film transducers<sup>228</sup>. Finally, of high relevance in biomedical applications is to further study biological effects triggered by acoustic actuation at the microscopic and nanoscopic length scales and at various time scales. For example, most studies so far have focused on demonstrating that the ultrasound used in acoustofluidic devices does not cause any noticeable effects on biological cells. However, there may be several advantageous effects of ultrasound exposure at the cellular and molecular level yet to be explored and demonstrated.

Although the use of acoustofluidics has expanded into multiple fields of research in biology and medicine, there are still many emerging areas where acoustofluidics can play a major role. Take, for example, the recent demonstrations of in vivo acoustic manipulation<sup>252</sup>. Although not considered a traditional application of acoustofluidics, the manipulation of biological objects within living tissue is in many ways similar to the manipulation of objects within microfluidic devices. Owing to their non-invasive nature and ability to penetrate deep into tissue, acoustic waves hold great potential as a non-surgical alternative for moving objects, such as kidney stones or robotic cameras, within the human body. In addition to contact-free

manipulation applications, in vivo acoustofluidic technologies can enable new possibilities in therapeutic areas such as neural stimulation and targeted drug delivery. By thinking of creative ways to apply microfluidic-based acoustofluidic concepts to in vivo applications, researchers can develop translational acoustofluidic technologies to address unmet clinical needs. Focusing on these clinical needs will foster the development of more practical acoustofluidic technologies and help acoustofluidic technologies transition from specialized research laboratories into clinics and hospitals.

Published online: 21 April 2022

- This comprehensive review article provides a thorough overview of the underlying physics of acoustofluidic technologies, with a particular emphasis placed on wave generation and propagation in solids and fluids.**
- Friend, J. & Yeo, L. Y. Microscale acoustofluidics: microfluidics driven via acoustics and ultrasonics. *Rev. Mod. Phys.* **83**, 647–704 (2011).
  - Bruus, H. et al. Forthcoming Lab on a Chip tutorial series on acoustofluidics: acoustofluidics-exploiting ultrasonic standing wave forces and acoustic streaming in microfluidic systems for cell and particle manipulation. *Lab Chip* **11**, 3579–3580 (2011).
  - Zhang, P., Bachman, H., Ozcelik, A. & Huang, T. J. Acoustic microfluidics. *Annu. Rev. Anal. Chem.* **13**, 17–43 (2020).
  - Ozcelik, A. et al. Acoustic tweezers for the life sciences. *Nat. Methods* **15**, 1021–1028 (2018). **This review paper provides an introduction to the various applications of acoustic tweezer technologies in the life sciences.**
  - Westervelt, P. J. The theory of steady forces caused by sound waves. *J. Acoust. Soc. Am.* **23**, 312–315 (1951).
  - Zhang, L. & Marston, P. L. Axial radiation force exerted by general non-diffracting beams. *J. Acoust. Soc. Am.* **131**, EL329–EL335 (2012).
  - Zhang, L. From acoustic radiation pressure to three-dimensional acoustic radiation forces. *J. Acoust. Soc. Am.* **144**, 443–447 (2018).
  - Marston, P. L. Axial radiation force of a Bessel beam on a sphere and direction reversal of the force. *J. Acoust. Soc. Am.* **120**, 3518–3524 (2006).
  - Brillouin, L. *Tensors in Mechanics and Elasticity* (Academic, 1964).
  - King, L. V. On the acoustic radiation pressure on spheres. *Proc. R. Soc. London. Ser. A Mathem. Phys. Sci.* **147**, 212–240 (1934).
  - Yosioka, K. & Kawasima, Y. Acoustic radiation pressure on a compressible sphere. *Acta Acust. U Acust.* **5**, 167–173 (1955).
  - Wei, W., Thiessen, D. B. & Marston, P. L. Acoustic radiation force on a compressible cylinder in a standing wave. *J. Acoust. Soc. Am.* **116**, 201–208 (2004).
  - Sapozhnikov, O. A. & Bailey, M. R. Radiation force of an arbitrary acoustic beam on an elastic sphere in a fluid. *J. Acoust. Soc. Am.* **133**, 661–676 (2013).
  - Doinikov, A. A. Acoustic radiation pressure on a compressible sphere in a viscous fluid. *J. Fluid Mech.* **267**, 1–22 (1994).
  - Doinikov, A. A. Acoustic radiation force on a spherical particle in a viscous heat-conducting fluid. I. General formula. *J. Acoust. Soc. Am.* **101**, 713–721 (1997).
  - Marston, P. L. & Zhang, L. Unphysical consequences of negative absorbed power in linear passive scattering: implications for radiation force and torque. *J. Acoust. Soc. Am.* **139**, 3139–3144 (2016).
  - Zhang, L. & Marston, P. L. Acoustic radiation force expressed using complex phase shifts and momentum-transfer cross sections. *J. Acoust. Soc. Am.* **140**, EL178–EL183 (2016).
  - Zhang, L. & Marston, P. L. Angular momentum flux of nonparaxial acoustic vortex beams and torques on axisymmetric objects. *Phys. Rev. E* **84**, 065601 (2011).
  - Silva, G. T. Acoustic radiation force and torque on an absorbing compressible particle in an inviscid fluid. *J. Acoust. Soc. Am.* **136**, 2405–2413 (2014).
  - Zhang, L. & Marston, P. L. Acoustic radiation torque on small objects in viscous fluids and connection with viscous dissipation. *J. Acoust. Soc. Am.* **136**, 2917–2921 (2014).
  - Karlsen, J. T. & Bruus, H. Forces acting on a small particle in an acoustical field in a thermoviscous fluid. *Phys. Rev. E* **92**, 043010 (2015).
  - Muller, P. B. & Bruus, H. Theoretical aspects of microchannel acoustofluidics: thermoviscous corrections to the radiation force and streaming. *Procedia IUTAM* **10**, 410–415 (2014).
  - Zhang, L. & Marston, P. L. Acoustic radiation torque and the conservation of angular momentum (L). *J. Acoust. Soc. Am.* **129**, 1679–1680 (2011).
  - Hahn, P., Lamrecht, A. & Dual, J. Numerical simulation of micro-particle rotation by the acoustic viscous torque. *Lab Chip* **16**, 4581–4594 (2016).
  - Zhang, L. Reversals of orbital angular momentum transfer and radiation torque. *Phys. Rev. Appl.* **10**, 034039 (2018).
  - Silva, G. T. An expression for the radiation force exerted by an acoustic beam with arbitrary waveform (L). *J. Acoust. Soc. Am.* **130**, 3541–3544 (2011).
  - Mitri, F. Acoustic radiation force acting on elastic and viscoelastic spherical shells placed in a plane standing wave field. *Ultrasonics* **43**, 681–691 (2005).
  - Hasegawa, T. & Yosioka, K. Acoustic-radiation force on a solid elastic sphere. *J. Acoust. Soc. Am.* **46**, 1139–1143 (1969).
  - Hasegawa, T., Saka, K., Inoue, N. & Matsuzawa, K. Acoustic radiation force experienced by a solid cylinder in a plane progressive sound field. *J. Acoust. Soc. Am.* **83**, 1770–1775 (1988).
  - Gong, Z. & Baudoin, M. Equivalence between angular spectrum-based and multipole expansion-based formulas of the acoustic radiation force and torque. *J. Acoust. Soc. Am.* **149**, 3469 (2021).
  - Cai, F., Meng, L., Jiang, C., Pan, Y. & Zheng, H. Computation of the acoustic radiation force using the finite-difference time-domain method. *J. Acoust. Soc. Am.* **128**, 1617–1622 (2010).
  - Cosgrove, J. A., Buick, J. M., Campbell, D. M. & Created, C. A. Numerical simulation of particle motion in an ultrasound field using the lattice Boltzmann model. *Ultrasonics* **43**, 21–25 (2004).
  - Wijaya, F. B. & Lim, K.-M. Numerical calculation of acoustic radiation force and torque acting on rigid non-spherical particles. *Acta Acust. United Acust.* **101**, 531–542 (2015).
  - Baasch, T., Pavlic, A. & Dual, J. Acoustic radiation force acting on a heavy particle in a standing wave can be dominated by the acoustic microstreaming. *Phys. Rev. E* **100**, 061102 (2019).
  - Doinikov, A. A. Acoustic radiation interparticle forces in a compressible fluid. *J. Fluid Mech.* **444**, 1–21 (2001).
  - Silva, G. T. & Bruus, H. Acoustic interaction forces between small particles in an ideal fluid. *Phys. Rev. E* **90**, 063007 (2014).
  - Sepehrirhnama, S. & Lim, K.-M. Generalized potential theory for close-range acoustic interactions in the Rayleigh limit. *Phys. Rev. E* **102**, 043307 (2020).
  - Bruus, H. Acoustofluidics 7: the acoustic radiation force on small particles. *Lab Chip* **12**, 1014–1021 (2012).
  - Gor'kov, L. P. On the forces acting on a small particle in an acoustical field in an ideal fluid. *Sov. Phys. Dokl.* **6**, 773–775 (1962).
  - Doinikov, A. A. Acoustic radiation forces: classical theory and recent advances. *Recent. Res. Dev. Acoust.* **1**, 39–67 (2003).
  - Baresch, D., Thomas, J.-L. & Marchiano, R. Observation of a single-beam gradient force acoustical trap for elastic particles: acoustical tweezers. *Phys. Rev. Lett.* **116**, 024301 (2016).
  - Jerome, T. S., Ilinskii, Y. A., Zabolotskaya, E. A. & Hamilton, M. F. Born approximation of acoustic radiation force and torque on soft objects of arbitrary shape. *J. Acoust. Soc. Am.* **145**, 36–44 (2019).
  - Lighthill, J. Acoustic streaming. *J. Sound. Vib.* **61**, 391–418 (1978).
  - Rayleigh, L. On the circulation of air observed in Kundt's tubes, and on some allied acoustical problems. *Philos. Trans. R. Soc. Lond.* **175**, 1–21 (1884).
  - Schllichting, H. Berechnung ebener periodischer Grenzschichtströmungen [Calculation of plane periodic boundary layer streaming]. *Z. für Physik* **33**, 327–335 (1932).
  - Eckart, C. Vortices and streams caused by sound waves. *Phys. Rev.* **73**, 68 (1948).
  - Nyborg, W. L. in *Acoustic Streaming* Vol. 2B Ch. 11 (eds Mason, W. P. & Thurston, R. N.) 265–329 (Academic, 1965).
  - Orosco, J. & Friend, J. Unraveling the complex dynamics of acoustofluidics. Preprint at <https://doi.org/10.48550/arXiv.2107.00172> (2021).
  - Chu, B.-T. & Apfel, R. E. Acoustic radiation pressure produced by a beam of sound. *J. Acoust. Soc. Am.* **72**, 1673–1687 (1982).
  - Bertelsen, A., Svards, A. & Tjøtta, S. Nonlinear streaming effects associated with oscillating cylinders. *J. Fluid Mech.* **59**, 493–511 (1973).
  - Vega, J. M., Rüdiger, S. & Viñals, J. Phenomenological model of weakly damped Faraday waves and the associated mean flow. *Phys. Rev. E* **70**, 046306 (2004).
  - Naugolnykh, K. & Ostrovsky, L. *Nonlinear Wave Processes in Acoustics* (Cambridge Univ. Press, 1998).
  - Zhang, N., Horesh, A., Manor, O. & Friend, J. Powerful acoustogeometric streaming from dynamic geometric nonlinearity. *Phys. Rev. Lett.* **126**, 164502 (2021).
  - Comnacher, W., Orosco, J. & Friend, J. Droplet ejection at controlled angles via acoustofluidic jetting. *Phys. Rev. Lett.* **125**, 184504 (2020).
  - Ding, X. et al. Cell separation using tilted-angle standing surface acoustic waves. *Proc. Natl. Acad. Sci. USA* **111**, 12992–12997 (2014).
  - Glynne-Jones, P. & Hill, M. Acoustofluidics 23: acoustic manipulation combined with other force fields. *Lab Chip* **13**, 1003–1010 (2013).
  - Collins, D. J., Alan, T. & Neild, A. Particle separation using virtual deterministic lateral displacement (vDL). *Lab Chip* **14**, 1595–1603 (2014).
  - Wiklund, M. et al. Ultrasonic standing wave manipulation technology integrated into a dielectrophoretic chip. *Lab Chip* **6**, 1537–1544 (2006).
  - Thalhammer, G. et al. Combined acoustic and optical trapping. *Biomed. Opt. Express* **2**, 2859–2870 (2011).
  - Dholakia, K., Drinkwater, B. W. & Ritsch-Marte, M. Comparing acoustic and optical forces for biomedical research. *Nat. Rev. Phys.* **2**, 480–491 (2020).
  - Akther, A., Marqus, S., Rezk, A. R. & Yeo, L. Y. Submicron particle and cell concentration in a closed chamber surface acoustic wave microcentrifuge. *Anal. Chem.* **92**, 10024–10032 (2020).
  - Liu, S. et al. Investigation into the effect of acoustic radiation force and acoustic streaming on particle patterning in acoustic standing wave fields. *Sensors* **17**, 1664 (2017).

63. Muller, P. B., Barnkob, R., Jensen, M. J. H. & Bruus, H. A numerical study of microparticle acoustophoresis driven by acoustic radiation forces and streaming-induced drag forces. *Lab Chip* **12**, 4617–4627 (2012).
64. Li, F. et al. Rapid acoustophoretic motion of microparticles manipulated by phononic crystals. *Appl. Phys. Lett.* **113**, 173503 (2018).
65. Barnkob, R., Augustsson, P., Laurell, T. & Bruus, H. Acoustic radiation- and streaming-induced microparticle velocities determined by microparticle image velocimetry in an ultrasound symmetry plane. *Phys. Rev. E* **86**, 056307 (2012).
66. Bruus, H. Acoustofluidics 10: scaling laws in acoustophoresis. *Lab Chip* **12**, 1578–1586 (2012).
67. Barnkob, R., Augustsson, P., Laurell, T. & Bruus, H. Measuring the local pressure amplitude in microchannel acoustophoresis. *Lab Chip* **10**, 563–570 (2010).
68. Leshot, A., Evander, M., Laurell, T. & Nilsson, J. Acoustofluidics 5: building microfluidic acoustic resonators. *Lab Chip* **12**, 684–695 (2012).
69. Friend, J. & Yeo, L. Y.-M. In *Encyclopedia of Microfluidics & Nanofluidics* Vol. 1 (ed. Li, D.) 1654–1662 (Springer, 2008).
70. Uchino, K. et al. Loss mechanisms and high power piezoelectrics. *J. Mater. Sci.* **41**, 217–228 (2006).
71. Zipparo, M. J., Shung, K. K. & Shrout, T. R. Piezoceramics for high-frequency (20 to 100 MHz) single-element imaging transducers. *IEEE Trans. Ultrason. Ferroelectr. Freq. Control* **44**, 1038–1048 (1997).
72. Zhou, Q., Lam, K. H., Zheng, H., Qiu, W. & Shung, K. K. Piezoelectric single crystal ultrasonic transducers for biomedical applications. *Prog. Mater. Sci.* **66**, 87–111 (2014).
73. Steckel, A. G., Bruus, H., Muralt, P. & Matlioub, R. Fabrication, characterization, and simulation of glass devices with AlN thin-film transducers for excitation of ultrasound resonances. *Phys. Rev. Appl.* **16**, 014014 (2021).
74. Dual, J., Hahn, P., Leibacher, I., Möller, D. & Schwarz, T. Acoustofluidics 6: experimental characterization of ultrasonic particle manipulation devices. *Lab Chip* **12**, 852–862 (2012).
75. Hawkes, J. J. & Radel, S. Acoustofluidics 22: multi-wavelength resonators, applications and considerations. *Lab Chip* **13**, 610–627 (2013).
76. Rezk, A. R., Tan, J. K. & Yeo, L. Y. HYbrid Resonant Acoustics (HYDRA). *Adv. Mater.* **28**, 1970–1975 (2016).
77. Melde, K., Mark, A. G., Qiu, T. & Fischer, P. Holograms for acoustics. *Nature* **537**, 518–522 (2016). **This study describes the use of 3D printed acoustic holograms to create complex, arbitrarily shaped acoustic fields that can be used to manipulate PDMS microspheres in water.**
78. Pereno, V. et al. Layered acoustofluidic resonators for the simultaneous optical and acoustic characterisation of cavitation dynamics, microstreaming, and biological effects. *Biomicrofluidics* **12**, 034109 (2018).
79. Ozer, M. B. & Cetin, B. An extended view for acoustofluidic particle manipulation: scenarios for actuation modes and device resonance phenomenon for bulk-acoustic-wave devices. *J. Acoust. Soc. Am.* **149**, 2802–2812 (2021).
80. Moisenenko, R. P. & Bruus, H. Whole-system ultrasound resonances as the basis for acoustophoresis in all-polymer microfluidic devices. *Phys. Rev. Appl.* **11**, 014014 (2019).
81. Leibacher, I., Schatz, S. & Dual, J. Impedance matched channel walls in acoustofluidic systems. *Lab Chip* **14**, 463–470 (2014).
82. Barani, A., Mosadeghi, P., Haghjooy Javanmard, S., Sepehrirahnama, S. & Sanati-Nezhad, A. Numerical and experimental analysis of a hybrid material acoustophoretic device for manipulation of microparticles. *Sci. Rep.* **11**, 22048 (2021).
83. Coakley, W. T., Bardsley, D. W., Grundy, M. A., Zamani, F. & Clarke, D. J. Cell manipulation in ultrasonic standing wave fields. *J. Chem. Technol. Biotechnol.* **44**, 43–62 (1989).
84. Barmatz, M. & Collas, P. Acoustic radiation potential on a sphere in plane, cylindrical, and spherical standing wave fields. *J. Acoust. Soc. Am.* **77**, 928–945 (1985).
85. Xu, D. et al. Acoustic manipulation of particles in a cylindrical cavity: theoretical and experimental study on the effects of boundary conditions. *Ultrasonics* **93**, 18–25 (2019).
86. Saito, M., Daian, T., Hayashi, K. & Izumida, S.-Y. Fabrication of a polymer composite with periodic structure by the use of ultrasonic waves. *J. Appl. Phys.* **83**, 3490–3494 (1998).
87. Li, J., Shen, C., Huang, T. J. & Cummer, S. A. Acoustic tweezer with complex boundary-free trapping and transport channel controlled by shadow waveguides. *Sci. Adv.* **7**, eabi5502 (2021).
88. Wu, J. Acoustical tweezers. *J. Acoust. Soc. Am.* **89**, 2140–2143 (1991). **This study presents the first demonstration of 3D particle trapping and movement using standing acoustic waves and is the namesake for acoustical tweezers.**
89. Tian, L. et al. Spontaneous assembly of chemically encoded two-dimensional coacervate droplet arrays by acoustic wave patterning. *Nat. Commun.* **7**, 13068 (2016).
90. Wang, T. et al. Particle manipulation with acoustic vortex beam induced by a brass plate with spiral shape structure. *Appl. Phys. Lett.* **109**, 123506 (2016).
91. Memoli, G. et al. Metamaterial bricks and quantization of meta-surfaces. *Nat. Commun.* **8**, 14608 (2017).
92. He, Z. et al. Acoustic transmission enhancement through a periodically structured stiff plate without any opening. *Phys. Rev. Lett.* **105**, 074301 (2010).
93. Xia, X. et al. Three-dimensional spiral motion of microparticles by a binary-phase logarithmic-spiral zone plate. *J. Acoust. Soc. Am.* **150**, 2401–2408 (2021).
94. Li, F. et al. Phononic-crystal-based acoustic sieve for tunable manipulations of particles by a highly localized radiation force. *Phys. Rev. Appl.* **1**, 051001 (2014).
95. Shen, Y.-X. et al. Ultrasonic super-oscillation wave-packets with an acoustic meta-lens. *Nat. Commun.* **10**, 3411 (2019).
96. Li, F. et al. Phononic-crystal-enabled dynamic manipulation of microparticles and cells in an acoustofluidic channel. *Phys. Rev. Appl.* **13**, 044077 (2020).
97. Bourquin, Y., Wilson, R., Zhang, Y., Reboud, J. & Cooper, J. M. Phononic crystals for shaping fluids. *Adv. Mater.* **23**, 1458–1462 (2011).
98. Yang, Y. et al. Self-navigated 3D acoustic tweezers in complex media based on time reversal. *Research* **2021**, 9781394 (2021).
99. Marzo, A. et al. Holographic acoustic elements for manipulation of levitated objects. *Nat. Commun.* **6**, 1–7 (2015).
100. Marzo, A. & Drinkwater, B. W. Holographic acoustic tweezers. *Proc. Natl Acad. Sci. USA* **116**, 84–89 (2019).
101. Ma, Z. et al. Spatial ultrasound modulation by digitally controlling microbubble arrays. *Nat. Commun.* **11**, 4537 (2020).
102. Wixforth, A. et al. Acoustic manipulation of small droplets. *Anal. Bioanal. Chem.* **379**, 982–991 (2004).
103. Ding, X. et al. Surface acoustic wave microfluidics. *Lab Chip* **13**, 3626–3649 (2013).
104. Destgeer, G. & Sung, H. J. Recent advances in microfluidic actuation and micro-object manipulation via surface acoustic waves. *Lab Chip* **15**, 2722–2738 (2015).
105. Connacher, W. et al. Micro/nano acoustofluidics: materials, phenomena, design, devices, and applications. *Lab Chip* **18**, 1952–1996 (2018).
106. Zhang, N. Q. & Friend, J. Fabrication of nanoheight channels incorporating surface acoustic wave actuation via lithium niobate for acoustic nanofluidics. *J. Vis. Exp.* **156**, e60648 (2020).
107. Mei, J. Y., Zhang, N. Q. & Friend, J. Fabrication of surface acoustic wave devices on lithium niobate. *J. Vis. Exp.* **160**, e61013 (2020).
108. Shilton, R., Tan, M. K., Yeo, L. Y. & Friend, J. R. Particle concentration and mixing in microdrops driven by focused surface acoustic waves. *J. Appl. Phys.* **104**, 014910 (2008).
109. Ding, X. et al. Tunable patterning of microparticles and cells using standing surface acoustic waves. *Lab Chip* **12**, 2491–2497 (2012).
110. Delsing, P. et al. The 2019 surface acoustic waves roadmap. *J. Phys. D Appl. Phys.* **52**, 353001 (2019).
111. Fu, Y. Q. et al. Engineering inclined orientations of piezoelectric films for integrated acoustofluidics and lab-on-a-chip operated in liquid environments. *Lab Chip* **21**, 254–271 (2021).
112. Shi, J. et al. Acoustic tweezers: patterning cells and microparticles using standing surface acoustic waves (SSAW). *Lab Chip* **9**, 2890–2895 (2009). **This study demonstrates the manipulation of particles and cells using surface acoustic waves.**
113. Riaud, A., Baudoin, M., Bou Matar, O., Becerra, L. & Thomas, J.-L. Selective manipulation of microscopic particles with precursor swirling Rayleigh waves. *Phys. Rev. Appl.* **7**, 024007 (2017).
114. Tian, Z. et al. Wave number-spiral acoustic tweezers for dynamic and reconfigurable manipulation of particles and cells. *Sci. Adv.* **5**, eaau6062 (2019).
115. Zhang, N., Mei, J., Gopesh, T. & Friend, J. Optimized, omnidirectional surface acoustic wave source: 152° Y-rotated cut of lithium niobate for acoustofluidics. *IEEE Trans. Ultrason. Ferroelectr. Freq. Control* **67**, 2176–2186 (2020).
116. Zhang, N. et al. Microliter ultrafast centrifuge platform for size-based particle and cell separation and extraction using novel omnidirectional spiral surface acoustic waves. *Lab Chip* **21**, 904–915 (2021).
117. Bach, J. S. & Bruus, H. Theory of pressure acoustics with viscous boundary layers and streaming in curved elastic cavities. *J. Acoust. Soc. Am.* **144**, 766–784 (2018).
118. Rezk, A. R., Manor, O., Yeo, L. Y. & Friend, J. R. Double flow reversal in thin liquid films driven by megahertz-order surface vibration. *Proc. R. Soc. A Math. Phys. Eng. Sci.* **470**, 20130765 (2014).
119. Meng, L. et al. Acoustic aligning and trapping of microbubbles in an enclosed PDMS microfluidic device. *Sens. Actuat. B Chem.* **160**, 1599–1605 (2011).
120. Travagliati, M. et al. Acoustofluidics and whole-blood manipulation in surface acoustic wave counterflow devices. *Anal. Chem.* **86**, 10633–10638 (2014).
121. Rezk, A. R., Yeo, L. Y. & Friend, J. R. Poloidal flow and toroidal particle ring formation in a sessile drop driven by megahertz order vibration. *Langmuir* **30**, 11243–11247 (2014).
122. Li, H., Friend, J. & Yeo, L. Surface acoustic wave concentration of particle and bioparticle suspensions. *Biomed. Microdevices* **28**, 4098–4104 (2007).
123. Nama, N. et al. Numerical study of acoustophoretic motion of particles in a PDMS microchannel driven by surface acoustic waves. *Lab Chip* **15**, 2700–2709 (2015).
124. Langelier, S. M., Yeo, L. Y. & Friend, J. UV epoxy bonding for enhanced SAW transmission and microscale acoustofluidic integration. *Lab Chip* **12**, 2970–2976 (2012).
125. Shi, J., Mao, X., Ahmed, D., Colletti, A. & Huang, T. J. Focusing microparticles in a microfluidic channel with standing surface acoustic waves (SSAW). *Lab Chip* **8**, 221–223 (2008).
126. Marston, P. L. Finite-size radiation force correction for inviscid spheres in standing waves. *J. Acoust. Soc. Am.* **142**, 1167 (2017).
127. Silva, G. T., Lopes, J. H., Leão-Neto, J. P., Nichols, M. K. & Drinkwater, B. W. Particle patterning by ultrasonic standing waves in a rectangular cavity. *Phys. Rev. Appl.* **11**, 054044 (2019).
128. Oberti, S., Neild, A. & Dual, J. Manipulation of micrometer sized particles within a micromachined fluidic device to form two-dimensional patterns using ultrasound. *J. Acoust. Soc. Am.* **121**, 778–785 (2007).
129. Lin, Q. et al. Trapping of sub-wavelength microparticles and cells in resonant cylindrical shells. *Appl. Phys. Lett.* **117**, 053501 (2020).
130. Baresch, D., Thomas, J.-L. & Marchiano, R. Spherical vortex beams of high radial degree for enhanced single-beam tweezers. *J. Appl. Phys.* **113**, 184901 (2013).
131. Jia, Y.-R. et al. Acoustic tweezing for both Rayleigh and Mie particles based on acoustic focused petal beams. *Appl. Phys. Lett.* **116**, 265504 (2020).
132. Baudoin, M. et al. Spatially selective manipulation of cells with single-beam acoustical tweezers. *Nat. Commun.* **11**, 4244 (2020). **This study demonstrates the selective manipulation of individual cells within a microfluidic chamber using acoustic vortices.**
133. Baresch, D. & Garbin, V. Acoustic trapping of microbubbles in complex environments and controlled payload release. *Proc. Natl Acad. Sci. USA* **117**, 15490–15496 (2020).
134. Andrade, M. A. B., Perez, N. & Adamowski, J. C. Review of progress in acoustic levitation. *Braz. J. Phys.* **48**, 190–213 (2018).

135. Xie, W. J. & Wei, B. Dependence of acoustic levitation capabilities on geometric parameters. *Phys. Rev. E* **66**, 026605 (2002).
136. Ide, T., Friend, J., Nakamura, K. & Ueha, S. A non-contact linear bearing and actuator via ultrasonic levitation. *Sens. Actuat. A Phys.* **135**, 740–747 (2007).
137. Drinkwater, B. W. A Perspective on acoustical tweezers—devices, forces, and biomedical applications. *Appl. Phys. Lett.* **117**, 180501 (2020).
138. Ma, Z., Collins, D. J., Guo, J. & Ai, Y. Mechanical properties based particle separation via traveling surface acoustic wave. *Anal. Chem.* **88**, 11844–11851 (2016).
139. Fan, X.-D. & Zhang, L. Trapping force of acoustical Bessel beams on a sphere and stable tractor beams. *Phys. Rev. Appl.* **11**, 014055 (2019).
140. Zhang, L. & Marston, P. L. Geometrical interpretation of negative radiation forces of acoustical Bessel beams on spheres. *Phys. Rev. E* **84**, 035601 (2011).
141. Xu, S. J., Qiu, C. Y. & Liu, Z. Y. Transversally stable acoustic pulling force produced by two crossed plane waves. *EPL* **99**, 44003 (2012).
142. Shi, J., Huang, H., Stratton, Z., Huang, Y. & Huang, T. J. Continuous particle separation in a microfluidic channel via standing surface acoustic waves (SSAW). *Lab Chip* **9**, 3354–3359 (2009).
143. Courtney, C. R. P. et al. Manipulation of particles in two dimensions using phase-controllable ultrasonic standing waves. *Proc. R. Soc. A Math. Phys. Eng. Sci.* **468**, 357–360 (2011).
144. Manneberg, O., Vanherberghen, B., Önfelt, B. & Wiklund, M. Flow-free transport of cells in microchannels by frequency-modulated ultrasound. *Lab Chip* **9**, 833–837 (2009).
145. Courtney, C. R. et al. Manipulation of microparticles using phase-controllable ultrasonic standing waves. *J. Acoust. Soc. Am.* **128**, EL195–EL199 (2010).
146. Ding, X. et al. On-chip manipulation of single microparticles, cells, and organisms using surface acoustic waves. *Proc. Natl Acad. Sci. USA* **109**, 11105–11109 (2012).
- This study demonstrates an acoustic manipulation method to precisely control a single microparticle, cell or organism along an arbitrary path in two dimensions.**
147. Meng, L. et al. On-chip targeted single cell sonoporation with microbubble destruction excited by surface acoustic waves. *Appl. Phys. Lett.* **104**, 073701 (2014).
148. Glynne-Jones, P., Boltryk, R. J. & Hill, M. Acoustofluidics 9: modelling and applications of planar resonant devices for acoustic particle manipulation. *Lab Chip* **12**, 1417–1426 (2012).
149. Augustsson, P., Karlsson, J. T., Su, H. W., Bruus, H. & Voldman, J. Iso-acoustic focusing of cells for size-insensitive acousto-mechanical phenotyping. *Nat. Commun.* **7**, 11556 (2016).
150. Destgeer, G., Ha, B. H., Jung, J. H. & Sung, H. J. Submicron separation of microspheres via travelling surface acoustic waves. *Lab Chip* **14**, 4665–4672 (2014).
151. Ren, L. et al. Standing surface acoustic wave (SSAW)-based fluorescence-activated cell sorter. *Small* **14**, 1801996 (2018).
152. Ren, L. et al. A high-throughput acoustic cell sorter. *Lab Chip* **15**, 3870–3879 (2015).
153. Mutafopolous, K. et al. Traveling surface acoustic wave (TSAW) microfluidic fluorescence activated cell sorter ( $\mu$ FACS). *Lab Chip* **19**, 2435–2443 (2019).
154. Tan, M., Friend, J. & Yeo, L. Microparticle collection and concentration via a miniature surface acoustic wave device. *Lab Chip* **7**, 618–625 (2007).
155. Collins, D. J., Ma, Z. & Ai, Y. Highly localized acoustic streaming and size-selective submicrometer particle concentration using high frequency microscale focused acoustic fields. *Anal. Chem.* **88**, 5513–5522 (2016).
156. Cui, W., Pang, W., Yang, Y., Li, T. & Duan, X. Theoretical and experimental characterizations of gigahertz acoustic streaming in microscale fluids. *Nanotechnol. Precis. Eng.* **2**, 15–22 (2019).
157. Li, H., Friend, J. R. & Yeo, L. Y. A scaffold cell seeding method driven by surface acoustic waves. *Biomaterials* **28**, 4098–4104 (2007).
158. Tan, M., Friend, J. & Yeo, L. Direct visualization of surface acoustic waves along substrates using smoke particles. *Appl. Phys. Lett.* **91**, 224101 (2007).
159. Miansari, M., Qi, A., Yeo, L. Y. & Friend, J. R. Vibration-induced deagglomeration and shear-induced alignment of carbon nanotubes in air. *Adv. Funct. Mater.* **25**, 1014–1023 (2015).
160. Hamilton, M. F., Ilinskii, Y. A. & Zabolotskaya, E. A. Acoustic streaming generated by standing waves in two-dimensional channels of arbitrary width. *J. Acoust. Soc. Am.* **113**, 153–160 (2003).
161. Tan, M. K., Tjeung, R., Ervin, H., Yeo, L. Y. & Friend, J. Double aperture focusing transducer for controlling microparticle motions in trapezoidal microchannels with surface acoustic waves. *Appl. Phys. Lett.* **95**, 134101 (2009).
162. Schneider, S. et al. Shear-induced unfolding triggers adhesion of von Willebrand factor fibers. *Proc. Natl Acad. Sci. USA* **104**, 7899–7903 (2008).
163. Raghavan, R. Theory for acoustic streaming in soft porous matter and its applications to ultrasound-enhanced convective delivery. *J. Therap. Ultrasound* **6**, 6 (2018).
164. Huang, A., Liu, H., Manor, O., Liu, P. & Friend, J. Enabling rapid charging lithium metal batteries via surface acoustic wave-driven electrolyte flow. *Adv. Mater.* **32**, 1907516 (2020).
165. Patel, M. V., Nanayakkara, I. A., Simon, M. G. & Lee, A. P. Cavity-induced microstreaming for simultaneous on-chip pumping and size-based separation of cells and particles. *Lab Chip* **14**, 3860–3872 (2014).
166. Kurashina, Y., Takemura, K. & Friend, J. Cell agglomeration in the wells of a 24-well plate using acoustic streaming. *Lab Chip* **17**, 876–886 (2017).
167. Mokhtare, A. et al. O-124 Contact-free oocyte denudation in a chip-scale ultrasonic microfluidic device. *Hum. Reprod.* **36** (Suppl. 1), deab1 26.049 (2021).
168. Iranmanesh, I. et al. Acoustic micro-vortexing of fluids, particles and cells in disposable microfluidic chips. *Biomed. Microdevices* **18**, 1–7 (2016).
169. Bussoniere, A., Baudoin, M., Brunet, P. & Matar, O. B. Dynamics of sessile and pendant drops excited by surface acoustic waves: gravity effects and correlation between oscillatory and translational motions. *Phys. Rev. E* **93**, 053106 (2016).
170. Baudoin, M., Brunet, P., Bou Matar, O. & Herth, E. Low power sessile droplets actuation via modulated surface acoustic waves. *Appl. Phys. Lett.* **100**, 154102 (2012).
171. Toegl, A., Kirchner, R., Gauer, C. & Wixforth, A. Enhancing results of microarray hybridizations through microagitation. *JBT* **14**, 197 (2003).
172. Combriat, T., Mekki-Berrada, F., Thibault, P. & Marmottant, P. Trapping and exclusion zones in complex streaming patterns around a large assembly of microfluidic bubbles under ultrasound. *Phys. Rev. Fluids* **3**, 013602 (2018).
173. Bertin, N. et al. Bubble-based acoustic micropropulsors: active surfaces and mixers. *Lab Chip* **17**, 1515–1528 (2017).
174. Wang, C., Rallabandi, B. & Hilgenfeldt, S. Frequency dependence and frequency control of microbubble streaming flows. *Phys. Fluids* **25**, 022002 (2013).
175. Doinikov, A. A. & Bouakaz, A. Acoustic microstreaming around a gas bubble. *J. Acoust. Soc. Am.* **127**, 703–709 (2010).
176. Marmottant, P. & Hilgenfeldt, S. A bubble-driven microfluidic transport element for bioengineering. *Proc. Natl Acad. Sci. USA* **101**, 9523–9527 (2004).
177. Huang, P.-H. et al. An acoustofluidic micromixer based on oscillating sidewall sharp-edges. *Lab Chip* **13**, 3847–3852 (2013).
178. Huang, P.-H. et al. A reliable and programmable acoustofluidic pump powered by oscillating sharp-edge structures. *Lab Chip* **14**, 4319–4323 (2014).
179. Zhang, N., Horesh, A. & Friend, J. Manipulation and mixing of 200 femtoliter droplets in nanofluidic channels using MHz-order surface acoustic waves. *Adv. Sci.* **8**, 2100408 (2021).
180. Guo, F. et al. Controlling cell–cell interactions using surface acoustic waves. *Proc. Natl Acad. Sci. USA* **112**, 43–48 (2015).
181. Guo, F. et al. Three-dimensional manipulation of single cells using surface acoustic waves. *Proc. Natl Acad. Sci. USA* **113**, 1522–1527 (2016).
182. Evander, M. et al. Noninvasive acoustic cell trapping in a microfluidic perfusion system for online bioassays. *Anal. Chem.* **79**, 2984–2991 (2007).
183. Hultström, J. et al. Proliferation and viability of adherent cells manipulated by standing-wave ultrasound in a microfluidic chip. *Ultrasound Med. Biol.* **33**, 145–151 (2007).
184. Collins, D. J. et al. Two-dimensional single-cell patterning with one cell per well driven by surface acoustic waves. *Nat. Commun.* **6**, 8686 (2015).
185. Courtney, C. R. et al. Dexterous manipulation of microparticles using Bessel-function acoustic pressure fields. *Appl. Phys. Lett.* **102**, 123508 (2013).
186. Baudoin, M. et al. Folding a focalized acoustical vortex on a flat holographic transducer: miniaturized selective acoustical tweezers. *Sci. Adv.* **5**, eaav1967 (2019).
187. Sitters, G. et al. Acoustic force spectroscopy. *Nat. Methods* **12**, 47–50 (2015).
- This study describes the development of an acoustofluidic technique for performing high-throughput measurements of single molecules and demonstrates its potential to study protein–protein and protein–DNA interactions.**
188. Sorkin, R. et al. Probing cellular mechanics with acoustic force spectroscopy. *Mol. Biol. Cell* **29**, 2005–2011 (2018).
189. Cartagena-Rivera, A. X., Van Itallie, C. M., Anderson, J. M. & Chadwick, R. S. Apical surface supracellular mechanical properties in polarized epithelium using noninvasive acoustic force spectroscopy. *Nat. Commun.* **8**, 1030 (2017).
190. Kamsma, D. et al. Single-cell acoustic force spectroscopy: resolving kinetics and strength of T cell adhesion to fibronectin. *Cell Rep.* **24**, 3008–3016 (2018).
191. Kamsma, D., Creyghton, R., Sitters, G., Wuite, G. J. & Peterman, E. J. Tuning the music: acoustic force spectroscopy (AFS) 2.0. *Methods* **105**, 26–33 (2016).
192. Baasch, T. et al. Acoustic compressibility of *Caenorhabditis elegans*. *Biophys. J.* **115**, 1817–1825 (2018).
193. Hyun, K.-A., Kim, J., Gwak, H. & Jung, H.-I. Isolation and enrichment of circulating biomarkers for cancer screening, detection, and diagnostics. *Analyst* **141**, 382–392 (2016).
194. Pantel, K. & Alix-Panabières, C. Circulating tumour cells in cancer patients: challenges and perspectives. *Trends Mol. Med.* **16**, 398–406 (2010).
195. Simpson, R. J., Lim, J. W., Moritz, R. L. & Mathivanan, S. Exosomes: proteomic insights and diagnostic potential. *Expert Rev. Proteom.* **6**, 267–283 (2009).
196. Augustsson, P., Magnusson, C., Nordin, M., Lilja, H. & Laurell, T. Microfluidic, label-free enrichment of prostate cancer cells in blood based on acoustophoresis. *Anal. Chem.* **84**, 7954–7962 (2012).
- This study shows the use of acoustofluidic technologies to isolate rare cancer cells from WBCs, demonstrating the potential of acoustofluidics in point-of-care diagnostics.**
197. Li, P. et al. Acoustic separation of circulating tumor cells. *Proc. Natl Acad. Sci. USA* **112**, 4970–4975 (2015).
198. Wu, M. et al. Circulating tumor cell phenotyping via high-throughput acoustic separation. *Small* **14**, 1801131 (2018).
199. Lee, K., Shao, H., Weissleder, R. & Lee, H. Acoustic purification of extracellular microvesicles. *ACS Nano* **9**, 2321–2327 (2015).
200. Wu, M. et al. Isolation of exosomes from whole blood by integrating acoustics and microfluidics. *Proc. Natl Acad. Sci. USA* **114**, 10584–10589 (2017).
201. Wang, Z. et al. Acoustofluidic separation enables early diagnosis of traumatic brain injury based on circulating exosomes. *Microsyst. Nanoeng.* **7**, 20 (2021).
202. Wang, Z. et al. Acoustofluidic salivary exosome isolation: a liquid biopsy compatible approach for human papillomavirus-associated oropharyngeal cancer detection. *J. Mol. Diagn.* **22**, 50–59 (2020).
203. Hammarström, B., Laurell, T. & Nilsson, J. Seed particle-enabled acoustic trapping of bacteria and nanoparticles in continuous flow systems. *Lab Chip* **12**, 4296–4304 (2012).
204. Rezeli, M. et al. Comparative proteomic analysis of extracellular vesicles isolated by acoustic trapping or differential centrifugation. *Anal. Chem.* **88**, 8577–8586 (2016).
205. Ku, A. et al. Acoustic enrichment of extracellular vesicles from biological fluids. *Anal. Chem.* **90**, 8011–8019 (2018).
206. Ku, A. et al. A urinary extracellular vesicle microRNA biomarker discovery pipeline: from automated extracellular vesicle enrichment by acoustic trapping to microRNA sequencing. *PLoS ONE* **14**, e0217507 (2019).
207. Zhang, S. P. et al. Digital acoustofluidics enables contactless and programmable liquid handling. *Nat. Commun.* **9**, 2928 (2018).
208. Franke, T., Braumüller, S., Schmid, L., Wixforth, A. & Weitz, D. Surface acoustic wave actuated cell sorting (SAWACS). *Lab Chip* **10**, 789–794 (2010).
209. Cho, S. H., Chen, C. H., Tsai, F. S., Godin, J. M. & Lo, Y.-H. Human mammalian cell sorting using a highly integrated micro-fluorinated fluorescence-activated cell sorter ( $\mu$ FACS). *Lab Chip* **10**, 1567–1573 (2010).
210. Zhang, J. et al. Fluorescence-based sorting of *Caenorhabditis elegans* via acoustofluidics. *Lab Chip* **20**, 1729–1739 (2020).

211. Lee, C.-Y., Chang, C.-L., Wang, Y.-N. & Fu, L.-M. Microfluidic mixing: a review. *Int. J. Mol. Sci.* **12**, 3263–3287 (2011).
212. Ozcelik, A. et al. An acoustofluidic micromixer via bubble inception and cavitation from microchannel sidewalls. *Anal. Chem.* **86**, 5083–5088 (2014).
213. Luong, T.-D., Phan, V.-N. & Nguyen, N.-T. High-throughput micromixers based on acoustic streaming induced by surface acoustic wave. *Microfluidics Nanofluidics* **10**, 619–625 (2011).
214. Gu, Y. et al. Acoustofluidic centrifuge for nanoparticle enrichment and separation. *Sci. Adv.* **7**, eabc0467 (2021).
215. Mao, Z. et al. Enriching nanoparticles via acoustofluidics. *ACS Nano* **11**, 603–612 (2017).
216. Cui, W. et al. Hypersonic-Induced 3D hydrodynamic tweezers for versatile manipulations of micro/nanoscale objects. *Part. Part. Syst. Charact.* **35**, 1800068 (2018).
217. Olofsson, K., Hammarström, B. & Wiklund, M. Ultrasonic based tissue modelling and engineering. *Micromachines* **9**, 594 (2018).
218. Olofsson, K. et al. Acoustic formation of multicellular tumor spheroids enabling on-chip functional and structural imaging. *Lab Chip* **18**, 2466–2476 (2018).
219. Chen, B. et al. High-throughput acoustofluidic fabrication of tumor spheroids. *Lab Chip* **19**, 1755–1763 (2019).
220. Armstrong, J. P. et al. Engineering anisotropic muscle tissue using acoustic cell patterning. *Adv. Mater.* **30**, 1802649 (2018).
221. Lata, J. P. et al. Surface acoustic waves grant superior spatial control of cells embedded in hydrogel fibers. *Adv. Mater.* **28**, 8632–8638 (2016).
222. Kang, B. et al. High-resolution acoustophoretic 3D cell patterning to construct functional collateral cylindroids for ischemia therapy. *Nat. Commun.* **9**, 5402 (2018). **This article demonstrates how acoustofluidic technologies can be used in practical tissue engineering applications by creating artificial tissues with acoustically aligned cells and implanting them into a mouse model.**
223. Gu, Y. et al. Acoustofluidic holography for micro-to nanoscale particle manipulation. *ACS Nano* **14**, 14635–14645 (2020).
224. Ma, Z. et al. Acoustic holographic cell patterning in a biocompatible hydrogel. *Adv. Mater.* **32**, 1904181 (2020).
225. Hagsäter, S. et al. Acoustic resonances in straight micro channels: beyond the 1D-approximation. *Lab Chip* **8**, 1178–1184 (2008).
226. Skov, N. R., Bach, J. S., Winckelmann, B. G. & Bruus, H. 3D modeling of acoustofluidics in a liquid-filled cavity including streaming, viscous boundary layers, surrounding solids, and a piezoelectric transducer. *Aims Mathem.* **4**, 99–111 (2019).
227. Bodé, W. N. & Bruus, H. Numerical study of the coupling layer between transducer and chip in acoustofluidic devices. *J. Acoust. Soc. Am.* **149**, 3096–3105 (2021).
228. Steckel, A. G. & Bruus, H. Numerical study of bulk acoustofluidic devices driven by thin-film transducers and whole-system resonance modes. *J. Acoust. Soc. Am.* **150**, 634–645 (2021).
229. Hammarström, B., Evander, M., Wahlström, J. & Nilsson, J. Frequency tracking in acoustic trapping for improved performance stability and system surveillance. *Lab Chip* **14**, 1005–1013 (2014).
230. Lickert, F., Ohlin, M., Bruus, H. & Olofsson, P. Acoustophoresis in polymer-based microfluidic devices: modeling and experimental validation. *J. Acoust. Soc. Am.* **149**, 4281–4291 (2021).
231. Tahmasebipour, A., Friedrich, L., Begley, M., Bruus, H. & Meinhart, C. Toward optimal acoustophoretic microparticle manipulation by exploiting asymmetry. *J. Acoust. Soc. Am.* **148**, 359–373 (2020).
232. Olofsson, K., Hammarström, B. & Wiklund, M. Acoustic separation of living and dead cells using high density medium. *Lab Chip* **20**, 1981–1990 (2020).
233. Qiu, W., Bruus, H. & Augustsson, P. Particle-size-dependent acoustophoretic motion and depletion of micro- and nano-particles at long timescales. *Phys. Rev. E* **102**, 013108 (2020).
234. Hammarström, B., Skov, N. R., Olofsson, K., Bruus, H. & Wiklund, M. Acoustic trapping based on surface displacement of resonance modes. *J. Acoust. Soc. Am.* **149**, 1445–1453 (2021).
235. Antfolk, M., Muller, P. B., Augustsson, P., Bruus, H. & Laurell, T. Focusing of sub-micrometer particles and bacteria enabled by two-dimensional acoustophoresis. *Lab Chip* **14**, 2791–2799 (2014).
236. Glynn-Jones, P., Boltryk, R. J., Harris, N. R., Cranny, A. W. & Hill, M. Mode-switching: a new technique for electronically varying the agglomeration position in an acoustic particle manipulator. *Ultrasonics* **50**, 68–75 (2010).
237. Jonnalagadda, U. S. et al. Acoustically modulated biomechanical stimulation for human cartilage tissue engineering. *Lab Chip* **18**, 473–485 (2018).
238. Bach, J. S. & Bruus, H. Suppression of acoustic streaming in shape-optimized channels. *Phys. Rev. Lett.* **124**, 214501 (2020).
239. Karlson, J. T., Qiu, W., Augustsson, P. & Bruus, H. Acoustic streaming and its suppression in inhomogeneous fluids. *Phys. Rev. Lett.* **120**, 054501 (2018).
240. Van Assche, D. et al. Gradient acoustic focusing of sub-micron particles for separation of bacteria from blood lysate. *Sci. Rep.* **10**, 3670 (2020).
241. Svennebring, J., Manneberg, O. & Wiklund, M. Temperature regulation during ultrasonic manipulation for long-term cell handling in a microfluidic chip. *J. Micromech. Microeng.* **17**, 2469 (2007).
242. Ohlin, M., Iranmanesh, I., Christakou, A. E. & Wiklund, M. Temperature-controlled MPa-pressure ultrasonic cell manipulation in a microfluidic chip. *Lab Chip* **15**, 3341–3349 (2015).
243. Cui, M., Kim, M., Weisensee, P. B. & Meacham, J. M. Thermal considerations for microswimmer trap-and-release using standing surface acoustic waves. *Lab Chip* **21**, 2534–2543 (2021).
244. Bazou, D., Kuznetsova, L. A. & Coakley, W. T. Physical environment of 2-D animal cell aggregates formed in a short pathlength ultrasound standing wave trap. *Ultrasound Med. Biol.* **31**, 423–430 (2005).
245. Apfel, R. E. & Holland, C. K. Gauging the likelihood of cavitation from short-pulse, low-duty cycle diagnostic ultrasound. *Ultrasound Med. Biol.* **17**, 179–185 (1991).
246. Wiklund, M. Acoustofluidics 12: biocompatibility and cell viability in microfluidic acoustic resonators. *Lab Chip* **12**, 2018–2028 (2012).
247. Tian, Z. et al. Generating multifunctional acoustic tweezers in Petri dishes for contactless, precise manipulation of bioparticles. *Sci. Adv.* **6**, eabb0494 (2020).
248. Bachman, H. et al. Open source acoustofluidics. *Lab Chip* **19**, 2404–2414 (2019).
249. Devendran, C., Carthew, J., Frith, J. E. & Neild, A. Cell adhesion, morphology, and metabolism variation via acoustic exposure within microfluidic cell handling systems. *Adv. Sci.* **6**, 1902326 (2019).
250. Li, H., Friend, J., Yeo, L., Dasvarma, A. & Traianedes, K. Effect of surface acoustic waves on the viability, proliferation and differentiation of primary osteoblast-like cells. *Biomicrofluidics* **3**, 034102 (2009).
251. Chen, C. et al. Acoustofluidic rotational tweezing enables high-speed contactless morphological phenotyping of zebrafish larvae. *Nat. Commun.* **12**, 1118 (2021).
252. Chameh, M. A. et al. Noninvasive acoustic manipulation of objects in a living body. *Proc. Natl. Acad. Sci. USA* **117**, 16848–16855 (2020).
253. Gracioso Martins, A. M. et al. Toward complete miniaturisation of flow injection analysis systems: microfluidic enhancement of chemiluminescent detection. *Anal. Chem.* **86**, 10812–10819 (2014).
254. Li, H., Friend, J. R. & Yeo, L. Y. Microfluidic colloidal island formation and erasure induced by surface acoustic wave radiation. *Phys. Rev. Lett.* **101**, 084502 (2008).
255. Huang, P.-H. et al. An acoustofluidic sputum liquefier. *Lab Chip* **15**, 3125–3131 (2015).
256. Wu, Z. et al. Scaffold-free generation of heterotypic cell spheroids using acoustofluidics. *Lab Chip* **21**, 3498–3508 (2021).

**Acknowledgements**

The authors acknowledge support from the National Institutes of Health (NIH) (U18TR003778, R01GM135486, UH3TR002978, R01GM141055, R01GM132603, R01HD103727 and R01NS115591), National Science Foundation (NSF) (ECCS-1807601 and ECCS-1542148), National Natural Science Foundation of China (11974372) (to F.C.) and W.M. Keck Foundation. They thank S. Yang, S. P. Zhang, R. Zhong and L. Zhang for helpful discussion.

**Author contributions**

Introduction (T.J.H., J.R., F.C. and J.F.); Experimentation (J.F., F.C., J.R. and T.J.H.); Results (F.C., J.F., J.R. and T.J.H.); Applications (T.J.H. and J.R.); Reproducibility and data deposition (M.W., J.R. and T.J.H.); Limitations and optimizations (M.W., J.R. and T.J.H.); Outlook (T.J.H., J.R. and M.W.); Overview of the Primer (T.J.H.).

**Competing interests**

T.J.H. has co-founded a start-up company, Ascent Bio-Nano Technologies Inc., to commercialize technologies involving acoustofluidics and acoustic tweezers. J.F. is a founding partner of Sonocharge Inc., commercializing acoustically driven rechargeable battery enhancement technology, and ARNAsystems Inc., commercializing rapid acoustofluidic diagnostic devices. J.R., F.C. and M.W. declare no competing interests.

**Peer review information**

*Nature Reviews Methods Primers* thanks Ye Ai, Helen Mulvana and the other, anonymous, reviewer(s) for their contribution to the peer review of this work.

**Publisher's note**

Springer Nature remains neutral with regard to jurisdictional claims in published maps and institutional affiliations.

**Supplementary information**

The online version contains supplementary material available at <https://doi.org/10.1038/s43586-022-00109-7>.

© Springer Nature Limited 2022